scientific reports

Check for updates

OPEN

Network pharmacology-based investigation of the pharmacological mechanisms of diosgenin in nonalcoholic steatohepatitis

Peiyuan Gu[1,2,6], Juan Chen[3,6], Jingxin Xin[1,2,4], Huiqi Chen[1,2], Ran Zhang[1,2], Dan Chen[5], Yuhan Zhang[1,2]✉ & Shanshan Shao[1,2]✉

The prevalence of nonalcoholic steatohepatitis (NASH) is rising annually, posing health and economic challenges, with limited treatments available. Diosgenin, a natural steroidal compound found in various plants, holds potential as a therapeutic candidate. Recent studies have confirmed diosgenin's anti-inflammatory and metabolism-modulating properties. However, its therapeutic effects on NASH and the underlying mechanisms are still unclear. This study aims to explore diosgenin's protective effects and pharmacological mechanisms against NASH using network pharmacology, molecular docking, and experimental validation. We gathered potential targets of diosgenin and NASH from various databases to generate protein-protein interaction (PPI) networks. GO and KEGG pathway enrichment analyses identified key targets and mechanisms. Molecular docking confirmed the binding capacity between diosgenin and core target proteins. Additionally, a NASH cell model was developed to validate the pharmacological effects of diosgenin. Our investigation identified nine key targets (ALB, AKT1, TP53, VEGFA, MAPK3, EGFR, STAT3, CASP3, IGF1) that interact with diosgenin. Molecular docking indicated potential bindings interactions, while enrichment analyses revealed that diosgenin may enhance fatty acid metabolism via the PI3K-Akt pathway. Cellular experiments confirmed that diosgenin activates this pathway, reduces SCD1 expression, and decreases triglyceride and IL-6 levels. Our study elucidates that diosgenin may ameliorate triglyceride deposition and inflammation through the PI3K-Akt pathway.

Keywords Nonalcoholic steatohepatitis, Diosgenin, Network pharmacology, PI3K-Akt, SCD1

With the global increase in the prevalence of metabolic syndrome, diabetesand obesity, the incidence of nonalcoholic fatty liver disease (NAFLD) has also increased dramatically, and NAFLD has become the most common type of chronic liver disease worldwide. Nonalcoholic steatohepatitis (NASH) is an aggressive inflammatory subtype of NAFLD associated with 5% or more hepatic steatosis, hepatocellular damage (ballooning) and inflammation, with or without fibrosis[1,2]. 20% of NASH can progress to cirrhosis[3] or even liver cancer[4], and ultimately become the leading cause of liver transplantation[3,5]. Hepatic steatosis, characterized by the accumulation of triglyceride vesicles in hepatocytes[2], arises from an imbalance between triglyceride supply and demand in the liver. This imbalance is attributed to heightened hepatic de novo lipogenesis, augmented fatty acid uptake, and decreased fatty acid beta-oxidation and triglyceride output[6,7]. The hepatic inflammatory response promotes liver fibrosis progression and is a key driver of cirrhosis[8]. Despite the dramatic public health

[1]Key Laboratory of Endocrine Glucose and Lipids Metabolism and Brain Aging, Ministry of Education; Department of Endocrinology, Shandong Provincial Hospital Affiliated to Shandong First Medical University, Jinan, Shandong, China. [2]Shandong Key Laboratory of Endocrine Metabolism and Aging, Jinan, Shandong, China. [3]Department of Endocrinology, Central Hospital Affiliated to Shandong First Medical University, Jinan, Shandong, China. [4]Department of Endocrinology, Shandong Provincial Hospital, Shandong University, Jinan, Shandong, China. [5]Department of Electrocardiographic, Shandong Provincial Hospital Affiliated to Shandong First Medical University, Jinan, Shandong, China. [6]Peiyuan Gu and Juan Chen have equally contributed to this work. ✉email: zyhan007@126.com; shaoshanshan11@126.com

concern that NASH poses, no effective therapeutic drugs have been approved for clinical use[9,10]. Consequently, there is a pressing need to explore novel and effective therapeutic strategies and drugs to address this growing health concern. In recent years, significant progress has been made in the study of traditional Chinese medicine (TCM) for the treatment of NASH, providing valuable insights for the development of NASH therapeutics. The active component vitexin from *Shan Zha* ameliorates NASH by significantly reducing hepatic macrophage infiltration and downregulating the expression of molecules associated with triglyceride synthesis[11]. Alisol A from *Ze Xie* alleviates steatohepatitis by inhibiting oxidative stress and stimulating autophagy via the AMPK/mTOR pathway[12], and Alisol B has been reported to reduce ROS levels and suppress inflammatory cytokine expression[13]. These findings highlight the potential of TCM in NASH treatment.

Diosgenin is a steroidal compound found naturally in the matrix of plants such as fenugreek and wild yam[14] that has anti-inflammatory, immunomodulatory, hypolipidemic, antiviral, antifungal, and anti-allergic effects[15,16]. In recent years, diosgenin has drawn increasing amounts of attention in the treatment of various metabolic diseases, including diabetes[17], osteoporosis[18], and hyperlipidemia[19]. Recently, diosgenin was shown to improve hepatic lipid metabolism[20] by interfering with cholesterol absorption and transport[21], inhibiting triglyceride synthesis, accelerating the breakdown of free fatty acids[22] and affecting liver-gut circulation[23]. Diosgenin has also been confirmed to exhibit anti-inflammatory effects by inhibiting inflammatory signals from macrophages[24] and significantly attenuating the inflammatory response in obese adipose tissue[25]. However, whether diosgenin has a therapeutic effect on NASH, an inflammatory subtype of NAFLD, remains unclear.

Network pharmacology, an emerging discipline based on systems biology theory, integrates various disciplines, such as polypharmacology, bioinformatics, and network analysis. In recent years, network pharmacology has been used to analyze the molecular associations between drugs and therapeutic objects from the overall perspective of the system level and biological network and to reveal the systemic pharmacological mechanism of drugs, serving as a guide for the development of new medicines and clinical therapy[26,27]. Therefore, this study aimed to screen the potential targets and signaling pathways of diosgenin in NASH using network pharmacology. Further validation through cytological experiments was conducted to elucidate diosgenin's effects on NASH and its pharmacological mechanisms.

Materials and methods

Network pharmacology analysis

Prediction of the action targets of diosgenin

We first used "diosgenin" as the search term to obtain the active target in the HERB database[28] (http://herb.ac.cn/). The 2D molecular structure formula of diosgenin was downloaded from the PubChem database[29] (https://pubchem.ncbi.nlm.nih.gov/) and retrieved from the PharmMapper database[30,31] (http://www.lilab-ecust.cn/pharmmapper/). Furthermore, potential targets were predicted from the SwissTargetPrediction database[32] (http://www.swisstargetprediction.ch/). All the obtained targets were normalized for information using the UniProt database[33] (https://www.uniprot.org/), which was subsequently subjected to gene name analysis. Subsequently, all the targets retrieved from the above databases were merged, and duplicate values were removed to obtain the active targets.

Identification of NASH-related targets

NASH-related targets were comprehensively gathered using the search terms "non-alcoholic steatohepatitis" and "nonalcoholic steatohepatitis". We searched the GeneCards database[34] (https://www.genecards.org), DisGeNET database[35] (http://www.disgenet.org), OMIM database[36] (http://www.omim.org), and TTD database[37] (http://db.idrblab.net) to identify putative targets. Finally, all the above targets were combined, and duplicate values were removed to obtain NASH-related targets.

Analysis of overlapping targets of diosgenin in NASH target mapping

The targets of the above two steps were imported into Venn mapping software[38] (http://www.bioinformatics.com.cn/static/others/jvenn/example.html) for visualization and mapping, after which the common targets were obtained. These targets are potential targets of diosgenin for the treatment of NASH.

GO and KEGG pathway enrichment analysis

The overlapping targets of diosgenin and NASH were imported into the DAVID database 6.8[39] (https://david.ncifcrf.gov/) for enrichment analysis of three aspects of GO enrichment: biological process (BP), molecular function (MF), and cellular component (CC) enrichment, as well as KEGG pathway enrichment[40]. The results were screened according to the criteria of a false discovery rate (FDR) < 0.05 and $P < 0.05$, and the top 10 pathways with the most highly enriched targets were selected for visualization via GO enrichment analysis and KEGG signaling pathway analysis via the "Microbiology Letter" tool[38] (http://www.bioinformatics.com.cn/).

PPI network construction

We submitted the overlapping targets to the STRING database[41] (https://string-db.org/) to predict functional protein association networks. For the protein–protein interaction (PPI) network constructed using the STRING database, the minimum interaction threshold was set to 0.4, with other parameters at default values. This generated a highly interconnected PPI network and derived combined PPI score data[42]. The composite score reflects protein interaction strength: higher scores indicate stronger interactions. The obtained network data were further imported into Cytoscape 3.7.2[43] (http://cytoscape.org/) software for the analysis of topological properties. The degree value indicates the number of direct interactions for a target, with higher values suggesting greater biological relevance and functional importance. Therefore, we used degree value analysis and ranking to screen the key targets of diosgenin in NASH.

Molecular docking validation of the binding capacity between diosgenin and targets

Protein structures were acquired from the RCSB Protein Data Bank (PDB) (Table 7). Use Pymol 2.3.0 to remove protein crystallization water and original ligands. Subsequently, import the protein structures into Autodock Tools (version 1.5.6) to add hydrogens, calculate charges, assign charges, specify atom types, and save the processed structures in the pdbqt format. The three-dimensional structure of diosgenin was retrieved from the PubChem database. This structure was subsequently imported into ChemBio3D Ultra 14.0 for energy minimization and saved in the mol2 format. The optimized diosgenin was then imported into Autodock Tools (version 1.5.6) to add hydrogens, calculate and assign charges, define rotatable bonds, and save in the pdbqt format. The molecular docking parameters of diosgenin with target proteins are shown in Table 7. Finally, Autodock Tools (version 1.5.6) was employed to compute the docking score, thereby assessing the degree of matching and docking activity between the target and its ligand. Based on prior studies, a binding affinity of less than −4.25 kcal/mol is indicative of binding activity; a score below −5.0 kcal/mol denotes enhanced binding activity; and a value lower than −7 kcal/mol implies robust docking interactions between the ligand and the target[44]. The binding model was visualized by PyMol 2.3.0.

Cell experiments

Construction and processing of cellular models

HepG2 cells (National Model and Characteristic Experimental Cell Resource Bank/Chinese Academy of Sciences Typical Culture Repository Committee Cell Bank, China), a human hepatocellular carcinoma cell line, were cultured in MEM containing 10% fetal bovine serum (FND500; Shanghai Excell Biological Technology Co., Ltd., China). To construct the NASH cell model, HepG2 cells were treated with free fatty acids (FFAs; containing a palmitic acid to oleic acid molar ratio of 1:2; palmitic acid, P5585; Sigma, USA; oleic acid, O1383; Sigma, USA). The experimental groups were as follows: (i) normal control group: treated with the solvent BSA only; (ii) NASH model group: treated with FFA only; (iii) NASH + diosgenin group: Diosgenin (D1634, Sigma, USA) was added after FFA stimulation; and (iv) BSA + diosgenin group: Diosgenin was added in addition to the BSA treatment.

Cell activity assessment

The cytotoxic effects of FFA and diosgenin on HepG2 cells were detected by a CCK-8 assay (CK12, Beiren Chemical Technology Co., Ltd., China). HepG2 cells were seeded in 96-well plates at a density of 1×10^4/well, and media containing different concentrations of FFA (0, 0.1, 0.2, 0.3, 0.4, 0.5 mM) or diosgenin (0, 5, 10, 25, 50, 100 μM) were added for 24 h. CCK8 reagent was subsequently added, and the mixture was incubated at 37 °C for 1–2 h. The absorbance at a wavelength of 450 nm was subsequently determined. Cell viability was calculated as a percentage relative to untreated controls.

Oil Red O staining

The cells were cultured in 6-well plates (3×10^5 cells/well), treated with FFA and diosgenin, rinsed with PBS and then fixed in paraformaldehyde for 30 min. The triglycerides were stained with Oil Red O staining solution (O0625, Sigma–Aldrich, USA), and the nuclei were stained with hematoxylin. After the slices were sealed with glycerol gelatin, the cells were observed under a microscope.

Measurement of cellular triglyceride (TG), total cholesterol (TC), and free cholesterol (FC) levels

The intracellular contents of TG, TC, and FC were determined according to the instructions in the kit (E1013-50/E1015-50/E1016-50; Beijing Pulley Gene Technology Co., Ltd., China).

Supernatant IL-6 determination

Enzyme-linked immunosorbent assays (ELISAs) were utilized to assess IL-6 levels in HepG2 cell culture supernatants following the instructions of an ELISA kit (EK106, UNIQUE Biologicals, China).

Western blot analysis

Cells were lysed using RIPA buffer, and total cellular proteins were extracted. Protein concentrations were determined with a BCA protein analysis kit. Proteins were separated by sodium dodecyl sulfate-polyacrylamide gel electrophoresis (SDS-PAGE). The proteins were subsequently transferred to PVDF membranes, blocked with 5% milk, and incubated with primary antibodies overnight at 4 °C. p-AKT (Ser473; #12694), AKT (#9272), FASN (#3180), ACC (#3676), and p-ACC (#11818) antibodies from CST; PI3K (PTM-635) from PTM Bio; CPT1α (Ab128569); SCD1 (Ab1986) from Abcam; and GAPDH (#66000) from Proteintech were used. The blots were incubated with secondary antibodies for 1 h at room temperature. An Alpha Q detection system (GE Healthcare) was used for visualization.

Statistical analysis

Statistical analysis was performed using GraphPad Prism 8.0 software. The data are expressed as the mean ± standard deviation (x ± sd), and one-way ANOVA was used for multiple comparisons between groups. A $P\ value < 0.05$ was considered statistically significant.

Results

Network of diosgenin targets in NASH treatment

A flow chart illustrating the methodology employed in this research is presented in Fig. 1. To elucidate the potential targets of diosgenin in the treatment of NASH, we first conducted a search in the HERB database, PharmMapper database, and SwissTargetPrediction database to determine the action targets of diosgenin; subsequently, all the obtained targets were combined, and duplicate values were deleted. Finally, 329 diosgenin

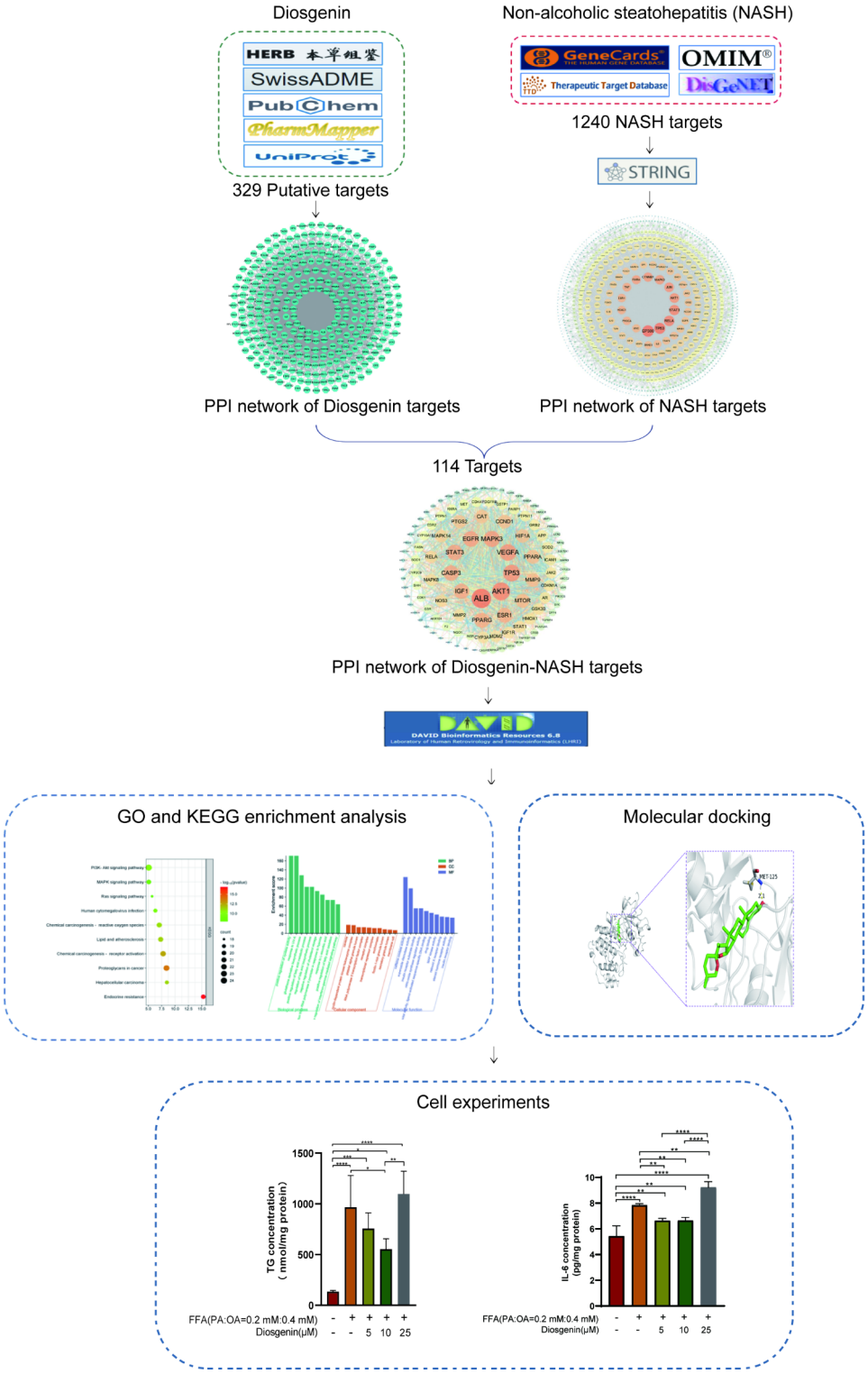

Fig. 1. Flow chart for studying the mechanism of diosgenin in NASH treatment.

action targets were obtained. A PPI network was constructed to analyze the relationships between diosgenin and its targets (Fig. 2).

The search terms "non-alcoholic steatohepatitis" and "nonalcoholic steatohepatitis" were used to identify genes in the GeneCards database, OMIM database, TTD database, and DisGeNET database. After removing duplicates, 1240 NASH-related targets were identified (Table 1). To identify the key targets of NASH, we constructed a PPI network and performed network topology analysis. The findings revealed that the 5 targets

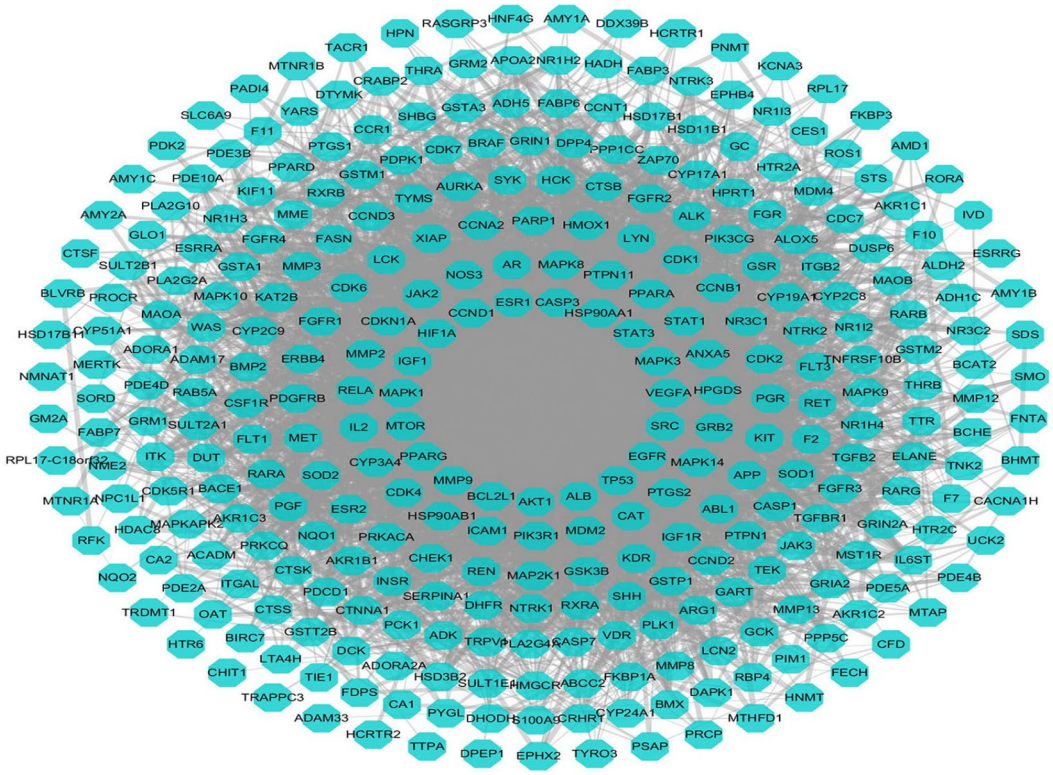

Fig. 2. Diosgenin-target network diagram.

with the highest degree values were EP300 (degree = 105), TP53 (degree = 100), RELA (degree = 91), STAT3 (degree = 89), and AKT1 (degree = 80) (Fig. 3).

Subsequently, mapping diosgenin targets ($n = 329$) to NASH targets ($n = 1240$) identified 114 overlapping targets (Table 2). Venn diagrams were generated for visualization purposes (Fig. 4A). The overlapping targets were imported into the STRING database to construct a PPI network. Additionally, network topology analysis was conducted using Cytoscape 7.3.2. As depicted in Fig. 4B, the PPI network contains a total of 114 nodes, and 9 key targets identified in the innermost circle based on the triple of the median degree value (≥ 57) are as follows: ALB (degree = 80), AKT1 (degree = 72), TP53 (degree = 66), VEGFA (degree = 64), MAPK3 (degree = 62), EGFR (degree = 59), STAT3 (degree = 59), CASP3 (degree = 58) and IGF1 (degree = 57). The above 9 targets are considered pivotal targets of diosgenin for NASH therapy.

GO and KEGG signaling pathway enrichment analysis

To further explore the potential mechanism of diosgenin in NASH treatment, an enrichment analysis of the 114 intersecting targets in the PPI network was performed employing the DAVID database. Using FDR < 0.05 and *p-value* < 0.05 as thresholds, 239 biological processes (BP), 32 cellular components (CC), and 66 molecular functions (MF) pathways were identified. The top 10 GO terms were ranked by Fold enrichment, and a bar graph was generated for visualization in Fig. 5A. The GO analysis revealed that the enriched BP pathways are primarily associated with metabolic regulation, oxidative stress and inflammation control (Table 3). The enriched CC pathways are mainly related to cell signaling, gene expression regulation and cellular secretion processes (Table 4). Meanwhile, the enriched MF pathways are predominantly involved in metabolic regulation, oxidative stress response, signal transduction, and gene expression regulation (Table 5). Among these, BP "positive regulation of fatty acid metabolic process (GO:0045923)" and "positive regulation of fatty acid oxidation (GO:0046321)" relate to Fatty acid metabolism, while BP "negative regulation of interferon-gamma-mediated signaling pathway (GO:0060336)," MF "superoxide dismutase activity (GO:0004784)," and "nitric-oxide synthase regulator activity (GO:0030235)" link to inflammation. Moreover, KEGG pathway enrichment analysis was performed to reveal the underlying signaling pathways involved. After removing the top 3 cancer-related pathways, the top 10 pathways were plotted in bubble diagrams according to the counts of hit targets and P values (Fig. 5B; Table 6). The primary pathway with the most enriched targets was the PI3K-Akt pathway (hsa04151). Based on this, we speculate that diosgenin could ameliorate fatty acid metabolism and inflammatory response in hepatocytes through the PI3K-Akt pathway to alleviate NASH progression.

Molecular docking results

To determine whether diosgenin can act on the nine core targets (ALB, AKT1, TP53, VEGFA, MAPK3, EGFR, STAT3, CASP3, IGF1), we conducted molecular docking studies. The results indicated that diosgenin exhibited binding affinity with all core targets. The other molecular docking results of diosgenin with target

Name	Name of protein	Degree	Betweenness centrality	Closeness centrality
EP300	Histone acetyltransferase p300	105	0.06059	0.43534
TP53	Cellular tumor antigen p53	100	0.072305	0.418318
RELA	Rela proto-oncogene, nf-kb subunit	91	0.051777	0.435583
STAT3	Signal transducer and activator of transcription 3	89	0.059363	0.422619
AKT1	RAC-alpha serine/threonine-protein kinase	80	0.043526	0.420797
JUN	Transcription factor AP-1	79	0.031724	0.425845
MAPK3	Mitogen-activated protein kinase 3	76	0.03821	0.415426
CTNNB1	Catenin beta-1	75	0.040032	0.408046
RXRA	Retinoic acid receptor RXR-alpha	70	0.047629	0.405083
TNF	Tumor necrosis factor	67	0.034141	0.410405
ESR1	Estrogen receptor	63	0.019721	0.407833
HDAC1	Histone deacetylase 1/2	62	0.023119	0.394444
PIK3CA	Phosphatidylinositol 4,5-bisphosphate 3-kinase catalytic subunit alpha isoform	62	0.013745	0.396648
MYC	Myc proto-oncogene protein	59	0.011523	0.401956
IL6	Interleukin-6	55	0.017332	0.400308
SMAD3	Mothers against decapentaplegic homolog 3	55	0.013719	0.38606
RPS27A	Ubiquitin-40 S ribosomal protein S27a	53	0.012557	0.380049
TRAF6	TNF receptor-associated factor 6	53	0.025533	0.363087
EGFR	Epidermal growth factor receptor	52	0.010025	0.392462
NFKB1	Nuclear factor NF-kappa-B p105 subunit	52	0.024978	0.394245
GRB2	Growth factor receptor-bound protein 2	51	0.015125	0.37476
JAK2	Tyrosine-protein kinase JAK2	51	0.012026	0.383031
NCOA1	Nuclear receptor coactivator 1	51	0.012763	0.380049
PTPN11	Tyrosine-protein phosphatase nonreceptor type 11	51	0.012051	0.382281
FOS	Proto-oncogene c-Fos	50	0.006847	0.380604
SHC1	SHC-transforming protein 1	50	0.008924	0.394843
PPARGC1A	Peroxisome proliferator-activated receptor gamma coactivator 1-alpha	49	0.023448	0.387978
NCOA2	Nuclear receptor coactivator 2	48	0.013544	0.373149
MAPK14	Mitogen-activated protein kinase 14	47	0.011388	0.398469
SP1	Transcription factor Sp1	47	0.014301	0.394245
FOXO1	Forkhead box protein O1	46	0.017711	0.395844
SMAD4	Mothers against decapentaplegic homolog 4	45	0.00857	0.381162
CAV1	Caveolin-1	43	0.01531	0.385489
FOXO3	Forkhead box protein O3	43	0.026149	0.393649
IL10	Interleukin-10	43	0.010475	0.391675
IL1B	Interleukin-1 beta	43	0.012489	0.380049
PPARA	Peroxisome proliferator-activated receptor alpha	43	0.00635	0.352278
HIF1A	Hypoxia-inducible factor 1-alpha	42	0.015371	0.371021
STAT1	Signal transducer and activator of transcription 1-alpha/beta	42	0.007944	0.386251
TLR4	Toll-like receptor 4	42	0.008126	0.393253
VEGFA	Vascular endothelial growth factor A	42	0.012763	0.383031
APOA1	Apolipoprotein A-I	41	0.028971	0.370493
CASP8	Caspase-8	39	0.003588	0.362413
CHUK	Inhibitor of nuclear factor kappa-B kinase subunit alpha	39	0.014676	0.364783
TGFB1	Transforming growth factor beta-1	39	0.013755	0.382843
FN1	Fibronectin 1	38	0.004889	0.370669
IRS1	Insulin receptor substrate 1	38	0.034125	0.365466
AR	Androgen receptor	37	0.010893	0.394046
IKBKB	Inhibitor of nuclear factor kappa-B kinase subunit beta	37	0.0039	0.356784
IKBKG	NF-kappa-B essential modulator	37	0.003234	0.357274
MAPK8	Mitogen-activated protein kinase 8/9/10 (c-jun n-terminal kinase)	37	0.007852	0.386634
CCND1	G1/S-specific cyclin-D1	36	0.009662	0.387401
PPARG	Peroxisome proliferator-activated receptor gamma	36	0.006206	0.37476
RIPK1	Receptor-interacting serine/threonine-protein kinase 1	36	0.003094	0.358257
CDKN1A	Cyclin-dependent kinase inhibitor 1	35	0.005917	0.369617
CXCL8	Interleukin-8	35	0.002845	0.375661
Continued				

Name	Name of protein	Degree	Betweenness centrality	Closeness centrality
CREB1	Cyclic AMP-responsive element-binding protein 1	34	0.009021	0.367357
MDM2	E3 ubiquitin-protein ligase Mdm2	34	0.007742	0.371374
MTOR	Serine/threonine-protein kinase mTOR	34	0.004772	0.38587
PRKCA	Protein kinase C alpha type	33	0.016424	0.371021
TNFRSF1A	Tumor necrosis factor receptor superfamily member 1 A	33	0.00471	0.365637
APOA2	Apolipoprotein A-II	32	0.011663	0.356296
LPL	Lipoprotein lipase	32	0.021649	0.355485
CASP3	Caspase-3	31	0.008417	0.365295
HGF	Hepatocyte growth factor	31	0.001757	0.343146
LIF	Lif, interleukin 6 family cytokine	31	0.006575	0.363087
BIRC3	Baculoviral IAP repeat-containing protein 3	30	0.004853	0.373684
IL4	Interleukin-4	30	0.014666	0.365637
SIRT1	NAD-dependent protein deacetylase sirtuin-1	30	0.006677	0.365979
YWHAZ	14-3-3 protein zeta/delta	30	0.001686	0.339565
APOE	Apolipoprotein E	29	0.007946	0.337365
CSF2	Granulocyte-macrophage colony-stimulating factor	29	0.009236	0.367876
INS	Insulin	29	0.004597	0.357929
PTEN	Phosphatase and tensin homolog	29	0.003939	0.364442
PTPN1	Tyrosine-protein phosphatase nonreceptor type 1	29	0.002263	0.35711
BIRC2	Baculoviral IAP repeat-containing protein 2	28	0.003464	0.355
CCL4	C-C motif chemokine 4	28	0.012084	0.362413
EGF	Pro-epidermal growth factor	28	0.003778	0.356296
IGF1	Insulin-like growth factor I	28	0.003406	0.372615
IGF1R	Insulin-like growth factor 1 receptor	28	0.004838	0.363256
IL1A	Interleukin-1 alpha	28	0.003337	0.366151
LEP	Leptin	28	0.01169	0.349597
MAP3K7	Mitogen-activated protein kinase kinase kinase 7	28	0.001717	0.336348
NR1H3	Oxysterols receptor LXR-alpha	28	0.001773	0.34991
UBE2D1	Ubiquitin-conjugating enzyme E2 D1	28	0.006291	0.358751
ATF2	Cyclic AMP-dependent transcription factor ATF-2	27	0.013327	0.365466
CCL2	C-C motif chemokine 2	27	0.005258	0.365295
CEBPB	CCAAT/enhancer-binding protein beta	27	0.011374	0.361742
CXCR4	C-X-C chemokine receptor type 4	27	0.001768	0.365466
GSK3B	Glycogen synthase kinase-3 beta	27	0.009884	0.352278
IRAK1	Interleukin-1 receptor-associated kinase 1	27	0.003	0.345728
PRKACA	cAMP-dependent protein kinase catalytic subunit alpha	27	0.002067	0.346341
SYK	Spleen associated tyrosine kinase	27	0.010146	0.356133
ACOX1	Peroxisomal acyl-coenzyme An oxidase 1	26	0.013433	0.355
APOB	Apolipoprotein B-100	26	0.006104	0.348194
CEBPA	CCAAT/enhancer-binding protein alpha	26	0.001805	0.371551
IRF7	Interferon regulatory factor 7	26	0.002043	0.370493
MYD88	Myeloid differentiation primary response protein MyD88	26	0.009959	0.305675
RPS6KB1	Ribosomal protein S6 kinase beta-1	26	0.003998	0.331072
ACTB	Actin, cytoplasmic 1	25	0.029931	0.343901
ALB	Serum albumin	25	0.011646	0.341794
ARRB1	Beta-arrestin-1	25	0.012045	0.355161
CCL5	C-C motif chemokine 5	25	0.004773	0.351485
EZH2	Histone-lysine N-methyltransferase EZH2	25	0.002717	0.365808
HMGB1	High mobility group protein B1	25	0.001531	0.351327
IL18	Interleukin-18	25	0.009815	0.356621
MMP1	Matrix metalloproteinase-1 (interstitial collagenase)	25	0.005839	0.362077
NCOA3	Nuclear receptor coactivator 3	25	0.007973	0.357601
PPP2CA	Serine/threonine-protein phosphatase 2 A catalytic subunit alpha isoform	25	0.005942	0.363933
PRKCD	Protein kinase C delta type	25	0.002079	0.347729
SMARCA4	Swi/snf related, matrix associated, actin dependent regulator of chromatin, subfamily a, member 4	25	0.003847	0.347884
SREBF1	Sterol regulatory element-binding protein 1	25	0.008203	0.334332
Continued				

Name	Name of protein	Degree	Betweenness centrality	Closeness centrality
CDK1	Cyclin-dependent kinase 1	24	0.001595	0.346495
CYP1A1	Cytochrome p450 family 1 subfamily a polypeptide 1	24	0.013317	0.282051
CYP2E1	Cytochrome P450 2E1	24	0.018464	0.312026
E2F1	Transcription factor E2F1	24	9.64E-04	0.343599
FASLG	Tumor necrosis factor ligand superfamily member 6	24	0.004117	0.337803
MMP9	Matrix metalloproteinase-9	24	0.006283	0.341794
PIK3CB	Phosphatidylinositol-4,5-bisphosphate 3-kinase catalytic subunit alpha/beta/delta	24	0.006443	0.334189
CYP3A4	Cytochrome p450 family 3 subfamily a polypeptide 4	23	0.003778	0.366839
HDAC3	Histone deacetylase 3	23	0.011185	0.370142
IFNG	Interferon gamma	23	0.004664	0.261729
IL17A	Interleukin-17 A	23	0.001892	0.353234
NOS2	Nitric-oxide synthase, inducible	23	0.004536	0.343599
SQSTM1	Sequestosome-1	23	0.002112	0.344356
TLR2	Toll-like receptor 2	23	0.001207	0.338095
AGT	Angiotensinogen	22	0.00649	0.350696
CD44	CD44 antigen	22	0.003654	0.348816
CXCL10	C-X-C motif chemokine 10	22	0.013108	0.327601
FAS	Tumor necrosis factor receptor superfamily member 6	22	0.008915	0.354034
PDGFRB	Platelet-derived growth factor receptor beta	22	0.00154	0.328981
PLG	Plasminogen	22	0.001496	0.336348
AXIN1	Axin-1	21	0.00809	0.355485
CD40	Tumor necrosis factor receptor superfamily member 5	21	0.009242	0.351169
F2	Prothrombin	21	0.001553	0.342544
HSPA4	Heat shock protein family A member 4	21	0.001426	0.345575
SDC1	Syndecan-1	21	0.006216	0.34835
TGFBR1	TGF-beta receptor type-1	21	0.011372	0.336928
APP	Amyloid-beta A4 protein	20	0.002587	0.337949
CCR5	C-C chemokine receptor type 5	20	0.01213	0.342094
CDK4	Cyclin-dependent kinase 4	20	0.002666	0.350381
GNAI2	Guanine nucleotide-binding protein G(i) subunit alpha-2	20	0.007359	0.362077
MET	Hepatocyte growth factor receptor	20	0.001112	0.342094
MMP2	Matrix metalloproteinase-2 (gelatinase a)	20	0.001642	0.335481
RAF1	RAF proto-oncogene serine/threonine-protein kinase	20	0.003045	0.357765
UBE2D2	Ubiquitin-conjugating enzyme E2 D2	20	0.002802	0.327738
APOA5	Apolipoprotein A-V	19	0.014329	0.331494
CAT	Catalase	19	0.005014	0.360739
CYCS	Cytochrome c, somatic	19	6.59E-04	0.352278
HSPA5	78 kDa glucose-regulated protein	19	0.012956	0.336348
IRF1	Interferon regulatory factor 1	19	0.005713	0.343901
IRS2	Insulin receptor substrate 2	19	0.002173	0.312901
MAP3K5	Mitogen-activated protein kinase kinase kinase 5	19	0.002898	0.341048
NOTCH1	Neurogenic locus notch homolog protein 1	19	0.013169	0.327326
OSM	Oncostatin-M	19	3.50E-04	0.332907
RUNX1	Runt-related transcription factor 1	19	6.44E-04	0.325281
APOC2	Apolipoprotein C-II	18	6.97E-04	0.349128
ARNT	Aryl hydrocarbon receptor nuclear translocator	18	8.02E-04	0.346495
BID	BH3-interacting domain death agonist	18	0.003645	0.356947
CPT1A	Carnitine O-palmitoyltransferase 1, liver isoform	18	0.006185	0.33234
IFNB1	Interferon beta	18	0.001196	0.307844
IL13	Interleukin-13	18	0.001304	0.332482
TICAM1	TIR domain-containing adapter molecule 1	18	7.14E-04	0.31748
BCL2	Apoptosis regulator Bcl-2	17	7.70E-04	0.315046
CCL3	C-C motif chemokine 3	17	0.002488	0.337511
CYP1A2	Cytochrome p450 family 1 subfamily a polypeptide 2	17	0.003391	0.350067
FABP1	Fatty acid-binding protein, liver	17	0.003809	0.362413
FOXP3	Forkhead box protein P3	17	0.002394	0.346495
Continued				

Name	Name of protein	Degree	Betweenness centrality	Closeness centrality
INSR	Insulin receptor	17	0.003206	0.363933
LBP	Lipopolysaccharide-binding protein	17	3.73E-04	0.335049
MAPK9	Mitogen-activated protein kinase 8/9/10 (c-jun n-terminal kinase)	17	0.001224	0.338388
NOS3	Nitric-oxide synthase, endothelial	17	8.90E-04	0.359908
NR1H2	Oxysterols receptor LXR-beta	17	5.50E-04	0.341645
PLAUR	Urokinase plasminogen activator surface receptor	17	0.001616	0.344812
PRKAA1	5'-AMP-activated protein kinase catalytic subunit alpha-1	17	0.002876	0.246761
RPTOR	Regulatory-associated protein of mTOR	17	8.12E-04	0.355971
RXRG	Retinoic acid receptor RXR-gamma	17	0.004379	0.336493
SAA1	Serum amyloid A-1 protein	17	0.003159	0.332058
SMAD7	Mothers against decapentaplegic homolog 7	17	1.69E-04	0.314539
SOCS3	Suppressor of cytokine signaling 3	17	4.18E-04	0.327601
TBP	TATA-box-binding protein	17	0.002204	0.323395
TERT	Telomerase reverse transcriptase	17	0.002049	0.351327
TGFBR2	Transforming growth factor beta receptor 2	17	0.011353	0.320608
TIMP1	Metalloproteinase inhibitor 1	17	3.78E-04	0.340453
AOX1	Aldehyde oxidase	16	0.001369	0.330652
ATM	Serine-protein kinase ATM	16	0.006589	0.261466
CD40LG	CD40 ligand	16	3.75E-04	0.342244
CDKN2A	Cyclin-dependent kinase inhibitor 2 A	16	0.002121	0.275582
CYP2B6	Cytochrome p450 family 2 subfamily b polypeptide 6	16	0.001511	0.324336
IL1R1	Interleukin-1 receptor type 1	16	7.46E-04	0.336783
IL6R	Interleukin-6 receptor subunit alpha	16	7.63E-04	0.338095
LCN2	Neutrophil gelatinase-associated lipocalin	16	4.32E-04	0.340899
PRKAG1	5'-AMP-activated protein kinase subunit gamma-1	16	4.34E-04	0.339713
STK11	Serine/threonine-protein kinase STK11	16	9.30E-04	0.334189
YAP1	Yes1 associated transcriptional regulator	16	7.62E-04	0.322328
ADIPOQ	Adiponectin, c1q and collagen domain containing	15	0.006522	0.341944
ATF4	Cyclic AMP-dependent transcription factor ATF-4	15	0.004779	0.336493
CD14	Monocyte differentiation antigen CD14	15	4.60E-04	0.306997
CETP	Cholesteryl ester transfer protein	15	0.002635	0.306756
IL6ST	Interleukin-6 receptor subunit beta	15	0.002196	0.333333
LDLR	Low-density lipoprotein receptor	15	4.04E-04	0.300616
PLIN1	Perilipin-1	15	3.31E-04	0.313907
RIPK3	Receptor-interacting serine/threonine-protein kinase 3	15	0.001985	0.327189
RUNX3	Runt-related transcription factor 3	15	1.79E-04	0.299119
TIRAP	Toll/interleukin-1 receptor domain-containing adapter protein	15	0.001781	0.353074
TNFRSF1B	Tumor necrosis factor receptor superfamily member 1B	15	0.002083	0.334619
ADRBK1	Beta-adrenergic receptor kinase 1	14	9.13E-04	0.328427
APOC3	Apolipoprotein C-III	14	8.65E-04	0.328013
ARID1A	AT-rich interactive domain-containing protein 1 A	14	0.003092	0.325688
ATG7	Ubiquitin-like modifier-activating enzyme ATG7	14	4.97E-04	0.350854
BIRC5	Baculoviral iap repeat-containing protein 5	14	0.00132	0.313152
BMP4	Bone morphogenetic protein 4	14	0.005492	0.319689
CASP6	Caspase-6	14	4.15E-04	0.254232
CASP7	Caspase-7	14	0.003764	0.326096
CTSD	Cathepsin D	14	0.003031	0.33234
CYP2A6	Cytochrome P450 2A6	14	0.003525	0.331072
DDIT3	DNA damage-inducible transcript 3 protein	14	0.003229	0.328565
DNMT1	DNA (cytosine-5)-methyltransferase 1	14	0.002138	0.331072
LRP6	Low-density lipoprotein receptor-related protein 6	14	5.27E-05	0.281543
MUC1	Mucin-1	14	5.68E-04	0.335481
PCNA	Proliferating cell nuclear antigen	14	9.57E-04	0.320739
PRKAA2	5'-AMP-activated protein kinase catalytic subunit alpha-2	14	0.002644	0.343901
PRKAB1	5'-AMP-activated protein kinase subunit beta-1	14	0.001289	0.33234
PSMD2	26 S proteasome non-ATPase regulatory subunit 2	14	3.64E-04	0.322328
Continued				

Name	Name of protein	Degree	Betweenness centrality	Closeness centrality
SERPINE1	Plasminogen activator inhibitor 1	14	2.76E-04	0.304009
STUB1	E3 ubiquitin-protein ligase CHIP	14	0.001266	0.343297
TLR3	Toll-like receptor 3	14	0.004725	0.343297
TNFSF10	Tumor necrosis factor ligand superfamily member 10	14	0.003242	0.329536
TXN	Thioredoxin	14	0.00339	0.352755
ABCA1	ATP-binding cassette subfamily A member 1	13	0.001789	0.334762
APOA4	Apolipoprotein A-IV	13	0.008703	0.338976
CCL19	C-C motif chemokine 19	13	6.57E-04	0.336348
CCNA2	Cyclin-A2	13	0.014638	0.285037
CD36	Platelet glycoprotein 4	13	0.003953	0.323798
EGR1	Early growth response protein 1	13	3.71E-04	0.279728
FGR	Fgr proto-oncogene, src family tyrosine kinase	13	0.0021	0.360074
HFE2	Hemojuvelin	13	4.40E-04	0.34375
HSPA1A	Heat shock protein family a member 1a	13	3.04E-04	0.318906
PSMD1	26 S proteasome non-ATPase regulatory subunit 1	13	0.002626	0.319166
PTGS2	Prostaglandin G/H synthase 2	13	8.35E-04	0.343146
RORA	Rar-related orphan receptor alpha	13	5.80E-04	0.325281
SMURF1	E3 ubiquitin-protein ligase SMURF1	13	0.003353	0.32596
THBS1	Thrombospondin-1	13	0.021624	0.346803
TNFAIP3	Tumor necrosis factor alpha-induced protein 3	13	0.008247	0.31215
TNFRSF10B	Tumor necrosis factor receptor superfamily member 10B	13	6.81E-04	0.329397
WNT3A	Wingless-type mmtv integration site family, member 3	13	0.001737	0.339713
ADRB2	Beta-2 adrenergic receptor	12	1.36E-04	0.303655
CASP9	Caspase-9	12	0.010175	0.310784
CFTR	Cystic fibrosis transmembrane conductance regulator	12	0.001665	0.318256
CYLD	Ubiquitin carboxyl-terminal hydrolase CYLD	12	0.012709	0.282766
CYP2C19	Cytochrome P450 2C19	12	0.005289	0.311031
CYP2C9	Cytochrome p450 family 2 subfamily c polypeptide 9	12	0.001245	0.306876
E2F2	Transcription factor E2F2	12	0.001081	0.333333
EIF2AK2	Interferon-induced, double-stranded RNA-activated protein kinase	12	7.89E-04	0.327052
ESR2	Estrogen receptor beta	12	7.90E-04	0.329119
GCG	Glucagon	12	0.009481	0.318776
GPIHBP1	Glycosylphosphatidylinositol-anchored high density lipoprotein-binding protein 1	12	0.001895	0.279628
HNF1A	Hepatocyte nuclear factor 1-alpha	12	0.00121	0.275194
HNF4A	Hepatocyte nuclear factor 4-alpha	12	1.16E-05	0.277837
ICAM1	Intercellular adhesion molecule 1	12	0.002659	0.277936
LAMA1	Laminin subunit alpha-1	12	8.66E-04	0.356621
LCAT	Phosphatidylcholine-sterol acyltransferase	12	9.78E-04	0.335481
LPA	Apolipoprotein(a)	12	2.32E-04	0.320476
MAOA	Amine oxidase [flavin-containing] A	12	0.008542	0.319558
NLRP3	NACHT, LRR and PYD domains-containing protein 3	12	1.18E-04	0.327189
NR0B2	Nuclear receptor subfamily 0 group B member 2	12	1.74E-04	0.341794
NR1H4	Bile acid receptor	12	0.004472	0.338829
PARP1	Poly [ADP-ribose] polymerase 1	12	0.001463	0.336783
RAB5A	RAB5A, member RAS oncogene family	12	0.001191	0.317867
SMPD1	Sphingomyelin phosphodiesterase	12	2.65E-04	0.347575
TFAP2A	Transcription factor ap-2 alpha/beta	12	0.001197	0.268477
XBP1	X-box-binding protein 1	12	0.001009	0.343297
CFLAR	CASP8 and FADD-like apoptosis regulator	11	4.26E-04	0.309184
DPP4	Dipeptidyl peptidase 4	11	7.18E-04	0.310908
EPHX1	Microsomal epoxide hydrolase	11	1.33E-04	0.328289
FASN	Fatty acid synthase	11	7.78E-04	0.333476
HMOX1	Heme oxygenase 1	11	0.011	0.344356
IL3	Interleukin-3	11	7.32E-04	0.345575
LGALS3	Galectin-3	11	6.97E-05	0.333903
PIK3CG	Phosphatidylinositol 4,5-bisphosphate 3-kinase catalytic subunit gamma isoform	11	3.54E-04	0.288192
Continued				

Name	Name of protein	Degree	Betweenness centrality	Closeness centrality
PIN1	Peptidyl-prolyl cis-trans isomerase NIMA-interacting 1	11	2.83E-04	0.336059
PLAU	Urokinase-type plasminogen activator	11	0.00207	0.308208
PLTP	Phospholipid transfer protein	11	4.74E-04	0.327601
PRKCQ	Protein kinase C theta type	11	0.00465	0.331072
PSME2	Proteasome activator subunit 2 (pa28 beta)	11	3.95E-04	0.326096
SHH	Sonic hedgehog protein	11	0.005794	0.330932
TCF7L2	Transcription factor 7-like 2	11	0.001886	0.314412
VDR	Vitamin D3 receptor	11	0.001104	0.322861
VIM	Vimentin	11	3.14E-04	0.257841
VTN	Vitronectin	11	0.001308	0.322994
APC	Adenomatous polyposis coli protein	10	5.52E-04	0.287661
ATF3	Cyclic AMP-dependent transcription factor ATF-3	10	0.005804	0.288511
CD28	T-cell-specific surface glycoprotein CD28	10	0.001868	0.299348
CLU	Clusterin	10	8.80E-04	0.337949
CXCR2	C-X-C chemokine receptor type 2	10	0.003524	0.32501
CYP2C8	Cytochrome p450 family 2 subfamily c polypeptide 8	10	0.003356	0.329119
CYP7A1	Cholesterol 7-alpha-monooxygenase	10	0.004325	0.337074
FABP4	Fatty acid-binding protein, adipocyte	10	5.79E-04	0.275
GADD45A	Growth arrest and DNA damage-inducible protein GADD45 alpha	10	3.48E-04	0.314792
HSPB1	Heat shock protein family b (small) member 1	10	1.84E-04	0.281239
IDH1	Isocitrate dehydrogenase [nadp] cytoplasmic	10	0.003707	0.302245
IL1RN	Interleukin-1 receptor antagonist protein	10	0.001224	0.32474
KLF4	Krueppel-like factor 4	10	0.003256	0.305436
LEPR	Leptin receptor	10	1.48E-04	0.333333
LMNA	Prelamin-A/C	10	0.005951	0.307844
MLXIPL	Carbohydrate-responsive element-binding protein	10	0.001866	0.322994
MLYCD	Malonyl-CoA decarboxylase, mitochondrial	10	9.97E-05	0.336203
NUP62	Nuclear pore glycoprotein p62	10	1.86E-04	0.293719
PKM	Pyruvate kinase m1/2	10	4.27E-06	0.293941
PON1	Serum paraoxonase/arylesterase 1	10	0.001338	0.302011
PRDX1	Peroxiredoxin-1	10	0.001659	0.317997
SOD1	Superoxide dismutase, cu-zn family	10	0.00789	0.32596
SOD2	Superoxide dismutase [Mn], mitochondrial	10	6.48E-04	0.330093
TLR6	Toll-like receptor 6	10	5.28E-04	0.347729
VCAM1	Vascular cell adhesion protein 1	10	0.005844	0.305915
VLDLR	Very low-density lipoprotein receptor	10	4.35E-04	0.323529
ACACA	Acetyl-CoA carboxylase 1	9	0.002775	0.272125
ACACB	Acetyl-CoA carboxylase 2	9	3.27E-04	0.274806
AHSG	Alpha-2-HS-glycoprotein	9	3.84E-04	0.298547
ALDH2	Aldehyde dehydrogenase, mitochondrial	9	0.005948	0.262081
ANXA2	Annexin A2	9	0.00464	0.314412
BAX	Apoptosis regulator BAX	9	0.001788	0.315046
BBC3	Bcl-2-binding component 3	9	9.93E-04	0.333191
CCR1	C-C chemokine receptor type 1	9	0.00504	0.315811
CLOCK	Circadian locomoter output cycles protein kaput	9	9.78E-04	0.326505
COL1A1	Collagen alpha-1(I) chain	9	0.004237	0.333476
CRP	C-reactive protein	9	0.003087	0.29494
CTLA4	Cytotoxic T-lymphocyte protein 4	9	0.004726	0.312026
CXCR3	C-X-C chemokine receptor type 3	9	0.001535	0.28023
DNMT3A	DNA (cytosine-5)-methyltransferase 3 A	9	3.02E-04	0.301777
DYNLL1	Dynein light chain 1, cytoplasmic	9	2.44E-04	0.289796
EIF2S1	Eukaryotic translation initiation factor 2 subunit 1	9	0.003174	0.296507
FAT1	Protocadherin Fat 1	9	4.21E-04	0.315556
GH1	Somatotropin	9	2.88E-04	0.294384
HP	Haptoglobin-related protein	9	0.002056	0.323798
KEAP1	Kelch-like ECH-associated protein 1	9	2.35E-04	0.316322
Continued				

Name	Name of protein	Degree	Betweenness centrality	Closeness centrality
LIPC	Hepatic triacylglycerol lipase	9	5.50E-04	0.311404
LRPPRC	Leucine-rich PPR motif-containing protein, mitochondrial	9	0.004222	0.3005
MMP7	Matrix metalloproteinase-7 (matrilysin, uterine)	9	6.50E-05	0.284517
NFE2L2	Nuclear factor erythroid 2-related factor 2	9	0.00131	0.303655
PNPLA2	Patatin-like phospholipase domain-containing protein 2	9	0.002018	0.314792
PRKDC	DNA-dependent protein kinase catalytic subunit	9	0.002852	0.311404
SREBF2	Sterol regulatory element-binding protein 2	9	2.73E-04	0.344356
SUFU	Suppressor of fused homolog	9	6.08E-04	0.337511
TFF3	Trefoil factor 3	9	0.002731	0.316322
ULK1	Serine/threonine-protein kinase ULK1	9	1.38E-05	0.341346
WNT5A	Wingless-type mmtv integration site family, member 5	9	1.99E-04	0.316836
WWTR1	WW domain-containing transcription regulator protein 1	9	0.003142	0.314412
ACVR2B	Activin receptor type-2B	8	0.001094	0.303419
CCR2	C-C chemokine receptor type 2	8	0.006279	0.275
COL3A1	Collagen alpha-1(III) chain	8	0.004506	0.311031
CTGF	Cellular communication network factor 2	8	2.74E-04	0.318386
CYP2J2	Cytochrome P450 2J2	8	0.002032	0.292948
ELAVL1	ELAV-like protein 1	8	2.41E-04	0.324201
ELK1	ETS domain-containing protein Elk-1	8	2.11E-04	0.316066
ENO1	Alpha-enolase	8	1.57E-04	0.316579
FDFT1	Squalene synthase	8	0.004483	0.253571
GHR	Growth hormone receptor	8	9.68E-04	0.291636
GHRL	Appetite-regulating hormone	8	4.82E-04	0.308696
GLUD1	Glutamate dehydrogenase 1, mitochondrial	8	0.003011	0.313403
GSK3A	Glycogen synthase kinase-3 alpha	8	5.82E-04	0.306876
HIST1H4F	Histone cluster 1 H4 family member f	8	0.002605	0.286395
HMGCR	3-hydroxy-3-methylglutaryl-coenzyme A reductase	8	0.002723	0.299923
HSD11B1	Corticosteroid 11-beta-dehydrogenase isozyme 1	8	8.33E-04	0.309798
IFNAR1	Interferon alpha/beta receptor 1	8	4.38E-04	0.29662
PDGFA	Platelet-derived growth factor subunit A	8	5.74E-05	0.283382
PIK3CD	Phosphatidylinositol 4,5-bisphosphate 3-kinase catalytic subunit delta isoform	8	0.006201	0.295386
PKLR	Pyruvate kinase PKLR	8	2.05E-04	0.323663
PLIN2	Perilipin-2	8	0.003818	0.308087
PPAP2B	Phosphatidate phosphatase	8	2.76E-04	0.265737
PPP1R15A	Protein phosphatase 1 regulatory subunit 15 A	8	3.44E-04	0.303066
PRKCE	Protein kinase C epsilon type	8	4.85E-05	0.323128
RB1CC1	RB1-inducible coiled-coil protein 1	8	7.88E-04	0.270617
SIRT3	NAD-dependent protein deacetylase sirtuin-3, mitochondrial	8	7.84E-05	0.308696
SPHK1	Sphingosine kinase 1	8	5.01E-04	0.303537
SPP1	Secreted phosphoprotein 1	8	0.006449	0.310784
TRIB3	Tribbles pseudokinase 3	8	5.61E-05	0.31215
VCP	Transitional endoplasmic reticulum ATPase	8	9.60E-04	0.301894
ACSL1	Long-chain-fatty-acid–CoA ligase 1	7	7.23E-04	0.316964
ADH1B	Alcohol dehydrogenase 1b (class i), beta polypeptide	7	2.50E-04	0.286395
AGTR1	Type-1 angiotensin II receptor	7	3.58E-04	0.300616
AHR	Aryl hydrocarbon receptor	7	0.003988	0.312026
ALDH1A1	Aldehyde dehydrogenase 1 family member a1	7	0.001207	0.31265
ATF6	Cyclic AMP-dependent transcription factor ATF-6 alpha	7	2.06E-04	0.238984
BRD4	Bromodomain-containing protein 4	7	5.78E-04	0.290767
C3	Complement C3	7	9.64E-04	0.329258
CXCL9	C-X-C motif chemokine 9	7	0.005562	0.279828
CYP17A1	Steroid 17-alpha-hydroxylase/17,20 lyase	7	5.25E-04	0.244751
CYP26B1	Cytochrome P450 26B1	7	8.19E-06	0.245675
CYP2D6	Cytochrome P450 2D6	7	0.002035	0.247074
DNMT3B	DNA (cytosine-5)-methyltransferase 3B	7	0.005486	0.306395
EEF1A1	Elongation factor 1-alpha 1	7	5.55E-05	0.336059
Continued				

Name	Name of protein	Degree	Betweenness centrality	Closeness centrality
EPAS1	Endothelial PAS domain-containing protein 1	7	8.61E-05	0.330372
FGFR4	Fibroblast growth factor receptor 4	7	1.66E-04	0.296507
GCLC	Glutamate–cysteine ligase catalytic subunit	7	0.006436	0.264746
GOT1	Aspartate aminotransferase, cytoplasmic	7	2.07E-05	0.279028
GSTM1	Glutathione S-transferase Mu 1	7	0.001221	0.280129
H6PD	GDH/6PGL endoplasmic bifunctional protein	7	0.004351	0.314539
LPIN1	Phosphatidate phosphatase LPIN1	7	6.23E-05	0.32447
NAMPT	Nicotinamide phosphoribosyltransferase	7	6.29E-04	0.262257
NNMT	Nicotinamide N-methyltransferase	7	0.002593	0.251692
PRSS1	Trypsin-1	7	0.006652	0.283279
RUVBL1	RuvB-like 1	7	3.54E-04	0.252017
SLC27A2	Very long-chain acyl-CoA synthetase	7	1.45E-04	0.32447
SLC2A4	Solute carrier family 2, facilitated glucose transporter member 4	7	7.51E-04	0.270617
USP7	Ubiquitin carboxyl-terminal hydrolase 7	7	0.001585	0.31265
ABCG1	ATP-binding cassette subfamily G member 1	6	1.57E-04	0.302713
ANGPTL3	Angiopoietin-related protein 3	6	0.007567	0.235738
ANXA1	Annexin A1	6	0	0.285662
BCL2A1	Bcl-2-related protein A1	6	0	0.300269
CDH2	Cadherin-2	6	1.67E-04	0.265646
CPT2	Carnitine O-palmitoyltransferase 2, mitochondrial	6	2.14E-04	0.295386
CSNK2B	Casein kinase II subunit beta	6	0.001561	0.287344
ECH1	Delta(3,5)-Delta(2,4)-dienoyl-CoA isomerase, mitochondrial	6	3.88E-04	0.311155
ELANE	Elastase, neutrophil expressed	6	2.47E-04	0.258011
ELOVL6	Elongation of very long-chain fatty acids protein 6	6	0.002777	0.302831
ERN1	Serine/threonine-protein kinase/endoribonuclease IRE1	6	2.06E-04	0.306997
FGF21	Fibroblast growth factor 21	6	1.60E-05	0.316451
GPI	Glucose-6-phosphate isomerase	6	6.30E-05	0.325824
HNRNPK	Heterogeneous nuclear ribonucleoprotein K	6	6.74E-04	0.274228
IFNA2	Interferon alpha-2	6	4.82E-04	0.320476
ITGA8	Integrin subunit alpha 8	6	1.11E-04	0.284
ITGAX	Integrin subunit alpha x	6	0.002804	0.278531
KHDRBS1	KH domain-containing, RNA-binding, signal transduction-associated protein 1	6	0.001804	0.312901
LIPE	Hormone-sensitive lipase	6	8.41E-05	0.324875
LOX	Protein-lysine 6-oxidase	6	4.36E-04	0.302596
MMP10	Matrix metalloproteinase-10 (stromelysin 2)	6	3.23E-06	0.220809
PF4	Platelet factor 4	6	0.001281	0.275097
PPARD	Peroxisome proliferator-activated receptor delta	6	0.004353	0.303891
PPIG	Peptidyl-prolyl cis-trans isomerase G	6	0.002472	0.269032
ROCK1	Rho-associated protein kinase 1	6	1.41E-04	0.296733
SCD	Stearoyl-coa desaturase (delta-9 desaturase)	6	6.54E-05	0.263406
SESN2	Sestrin-2	6	8.91E-05	0.320345
SULT2A1	Sulfotransferase family 2a member 1	6	8.79E-04	0.284103
TFRC	Transferrin receptor protein 1	6	6.33E-05	0.29889
TIMP2	Metalloproteinase inhibitor 2	6	2.54E-04	0.309429
TLR9	Toll-like receptor 9	6	5.80E-05	0.259814
TP53BP1	TP53-binding protein 1	6	1.20E-04	0.268108
ABHD5	1-acylglycerol-3-phosphate O-acyltransferase ABHD5	5	1.16E-04	0.294828
AGER	Advanced glycosylation end product-specific receptor	5	7.77E-04	0.259038
ATG3	Ubiquitin-like-conjugating enzyme ATG3	5	3.94E-04	0.264566
CCK	Cholecystokinin	5	5.03E-04	0.316066
CIDEC	Cell death inducing dffa like effector c	5	0.002996	0.297978
CNR1	Cannabinoid receptor 1	5	0.002743	0.302713
CP	Ceruloplasmin	5	0.005791	0.271841
CSF1	Macrophage colony-stimulating factor 1	5	5.18E-04	0.287132
CYBA	Cytochrome b-245, alpha polypeptide	5	7.89E-04	0.320476
CYP19A1	Aromatase	5	0.002287	0.282051
Continued				

Name	Name of protein	Degree	Betweenness centrality	Closeness centrality
DGAT1	Diacylglycerol O-acyltransferase 1	5	6.22E-05	0.261817
DROSHA	Ribonuclease 3	5	0.005159	0.270429
ELN	Elastin	5	2.92E-05	0.264836
FBXW7	F-box/WD repeat-containing protein 7	5	4.13E-04	0.299119
FGF19	Fibroblast growth factor 19	5	8.46E-05	0.305915
G6PC	Glucose-6-phosphatase	5	2.50E-04	0.287555
GIP	Gastric inhibitory polypeptide	5	5.09E-04	0.289152
GPS2	G protein pathway suppressor 2	5	0.001438	0.270242
GPX1	Glutathione peroxidase 1	5	3.21E-04	0.289152
GSR	Glutathione reductase, mitochondrial	5	0.002576	0.274806
IFIH1	Interferon-induced helicase C domain-containing protein 1	5	3.97E-04	0.293058
IGF2R	Cation-independent mannose-6-phosphate receptor	5	1.36E-05	0.30484
INSIG1	Insulin-induced gene 1 protein	5	2.14E-05	0.307359
LMNB1	Lamin-B1	5	0.002829	0.270617
LOXL1	Lysyl oxidase-like protein 1	5	2.81E-04	0.231751
LOXL2	Lysyl oxidase homolog 2	5	2.81E-04	0.231751
LUM	Lumican	5	3.82E-04	0.254646
MAP1LC3B	Microtubule-associated proteins 1 A/1B light chain 3B	5	4.57E-05	0.294051
MAP3K11	Mitogen-activated protein kinase kinase kinase 11	5	3.24E-05	0.316964
MMP13	Matrix metalloproteinase-13 (collagenase 3)	5	3.44E-05	0.318906
MPO	Myeloperoxidase	5	2.68E-04	0.293499
NPY	Pro-neuropeptide Y	5	0.002951	0.300269
NR5A2	Nuclear receptor subfamily 5 group A member 2	5	9.86E-04	0.245829
PCOLCE	Procollagen C-endopeptidase enhancer 1	5	2.40E-04	0.313277
PCSK9	Proprotein convertase subtilisin/kexin type 9	5	0.005266	0.263762
PHB	Prohibitin 1	5	0.002928	0.276656
PINK1	Serine/threonine-protein kinase PINK1, mitochondrial	5	6.55E-06	0.219136
POLR2D	DNA-directed RNA polymerase II subunit RPB4	5	6.55E-06	0.219136
PYCARD	Apoptosis-associated speck-like protein containing a CARD	5	1.07E-05	0.256823
SIRT6	NAD-dependent protein deacetylase sirtuin-6	5	0.002575	0.274228
TALDO1	Transaldolase 1	5	1.34E-04	0.311776
THRB	Thyroid hormone receptor beta	5	3.74E-04	0.303655
TLL1	Tolloid-like protein 1	5	0.00124	0.304483
TNFSF13B	Tumor necrosis factor ligand superfamily member 13B	5	6.01E-04	0.303537
TP53BP2	Apoptosis-stimulating of p53 protein 2	5	5.22E-04	0.320608
TTR	Transthyretin	5	8.54E-06	0.261117
UQCRB	Cytochrome b-c1 complex subunit 7	5	1.41E-05	0.291309
USF1	Upstream stimulatory factor 1	5	1.02E-06	0.294828
AATF	Apoptosis antagonizing transcription factor	4	0.001059	0.286606
ABCB4	Phosphatidylcholine translocator ABCB4	4	1.41E-05	0.282153
ACADM	Medium-chain specific acyl-CoA dehydrogenase, mitochondrial	4	0	0.297071
ACAT1	Acetyl-CoA acetyltransferase, mitochondrial	4	1.39E-05	0.264477
ADAMTS5	A disintegrin and metalloproteinase with thrombospondin motifs 5	4	0	0.297071
ADH1A	Alcohol dehydrogenase 1a (class i), alpha polypeptide	4	2.94E-04	0.245212
ADH1C	Alcohol dehydrogenase 1c (class i), gamma polypeptide	4	9.57E-05	0.256402
ADH4	Alcohol dehydrogenase 4 (class ii), pi polypeptide	4	3.74E-05	0.229841
AFP	Alpha-fetoprotein	4	3.74E-05	0.229841
AHCY	Adenosylhomocysteinase	4	5.73E-05	0.2384
ASS1	Argininosuccinate synthase	4	1.71E-04	0.307844
ATP5B	ATP synthase subunit beta, mitochondrial	4	0.002589	0.262786
BGLAP	Osteocalcin	4	6.11E-04	0.28629
CCL4L1	C-C motif chemokine 4-like	4	3.93E-04	0.282051
CD163	Scavenger receptor cysteine-rich type 1 protein M130	4	0	0.249521
CEACAM1	Carcinoembryonic antigen-related cell adhesion molecule 1	4	0	0.249521
CES1	Liver carboxylesterase 1	4	9.05E-05	0.307238
CPB2	Carboxypeptidase B2	4	6.82E-05	0.309307
Continued				

Name	Name of protein	Degree	Betweenness centrality	Closeness centrality
CYBB	Cytochrome b-245 heavy chain	4	5.32E-04	0.277541
DGAT2	Diacylglycerol O-acyltransferase 2	4	0.00253	0.278431
DKK1	Dickkopf-related protein 1	4	4.04E-04	0.262081
DRD2	D(2) dopamine receptor	4	0	0.274324
EHMT1	[histone h3]-lysine9 n-trimethyltransferase ehmt	4	3.47E-04	0.284517
ENPP1	Ectonucleotide pyrophosphatase/phosphodiesterase family member 1	4	4.51E-04	0.279528
FST	Follistatin	4	0.003299	0.285141
GATAD2A	Transcriptional repressor p66-alpha	4	0.002606	0.245907
GLP1R	Glucagon-like peptide 1 receptor	4	0.005437	0.300269
GPT	Glutamic–pyruvic transaminase	4	9.10E-05	0.286185
GSTP1	Glutathione S-transferase P	4	9.37E-05	0.245443
HAMP	Hepcidin	4	1.52E-04	0.280632
HFE	Hereditary hemochromatosis protein	4	2.19E-05	0.280029
IDH2	Isocitrate dehydrogenase [NADP], mitochondrial	4	3.60E-04	0.296395
IL27	Interleukin-27 subunit alpha	4	2.52E-04	0.252506
INSIG2	Insulin-induced gene 2 protein	4	1.49E-05	0.282153
KLB	Beta-klotho	4	7.20E-04	0.315939
KRT8	Keratin, type II cytoskeletal 8	4	8.55E-04	0.237747
MAT1A	S-adenosylmethionine synthase isoform type-1	4	5.59E-04	0.301777
MEIS1	Homeobox protein Meis1	4	3.08E-04	0.247152
MST1	Hepatocyte growth factor-like protein	4	5.68E-06	0.318386
MT-CYB	Cytochrome b	4	0	0.294495
MTTP	Microsomal triglyceride transfer protein large subunit	4	2.42E-06	0.308452
NDUFA13	NADH dehydrogenase [ubiquinone] 1 alpha subcomplex subunit 13	4	5.80E-05	0.316066
NR1I2	Nuclear receptor subfamily 1 group I member 2	4	0.001109	0.313403
NR1I3	Nuclear receptor subfamily 1 group I member 3	4	0.00175	0.299463
PLA2G4A	Cytosolic phospholipase A2	4	8.77E-04	0.308696
PNPLA3	Patatin-like phospholipase domain-containing protein 3	4	3.44E-05	0.243606
RETN	Resistin	4	2.80E-05	0.305197
S100A9	Protein S100-A9	4	0	0.325281
SCAP	Sterol regulatory element-binding protein cleavage-activating protein	4	1.76E-04	0.320608
SCARB1	Scavenger receptor class B member 1	4	0	0.309921
SELE	E-selectin	4	3.69E-04	0.296507
SERPINA1	Alpha-1-antitrypsin	4	2.83E-06	0.294162
SH2B1	SH2B adapter protein 1	4	2.73E-04	0.222825
SNAI2	Zinc finger protein SNAI2	4	3.63E-05	0.22359
SPARC	SPARC	4	0	0.305675
STK24	Serine/threonine-protein kinase 24	4	3.48E-06	0.260247
TOMM20	Mitochondrial import receptor subunit TOM20 homolog	4	3.48E-06	0.260247
TREM2	Triggering receptor expressed on myeloid cells 2	4	0	0.273364
TXNIP	Thioredoxin-interacting protein	4	0.002573	0.26628
USF2	Upstream stimulatory factor 2	4	2.04E-04	0.311652
USP18	Ubl carboxyl-terminal hydrolase 18	4	0.005257	0.298776
ABCB11	Atp-binding cassette, subfamily b (mdr/tap), member 11	3	0.00188	0.241273
ACO1	Cytoplasmic aconitate hydratase	3	0.002692	0.244674
ACSL4	Long-chain-fatty-acid–CoA ligase 4	3	8.28E-04	0.228096
ACTA2	Actin, aortic smooth muscle	3	1.86E-05	0.263851
ADAMTS13	A disintegrin and metalloproteinase with thrombospondin motifs 13	3	4.64E-04	0.304959
ADAMTSL2	ADAMTS-like protein 2	3	7.74E-05	0.285245
AIFM1	Apoptosis-inducing factor 1, mitochondrial	3	4.92E-04	0.287979
ALDH4A1	Delta-1-pyrroline-5-carboxylate dehydrogenase, mitochondrial	3	1.04E-04	0.26403
ANGPT2	Angiopoietin-2	3	6.49E-05	0.252098
AOC3	Amine oxidase, copper containing 3	3	0	0.253489
ARC	Activity-regulated cytoskeleton-associated protein	3	0	0.253489
AREG	Amphiregulin	3	9.46E-05	0.258781
BMP6	Bone morphogenetic protein 6	3	1.74E-06	0.269589
Continued				

Name	Name of protein	Degree	Betweenness centrality	Closeness centrality
C19orf80	Angiopoietin-like protein 8	3	1.77E-04	0.307238
CCL21	C-C motif chemokine 21	3	4.07E-04	0.213271
CD38	ADP-ribosyl cyclase/cyclic ADP-ribose hydrolase 1	3	4.87E-05	0.227498
CDKN3	Cyclin-dependent kinase inhibitor 3	3	2.93E-05	0.205689
CEACAM5	Carcinoembryonic antigen-related cell adhesion molecule 5	3	1.64E-06	0.203332
COX6B1	Cytochrome c oxidase subunit 6B1	3	9.40E-07	0.304246
CPS1	Carbamoyl-phosphate synthase [ammonia], mitochondrial	3	0	0.262698
CTRC	Chymotrypsin-C	3	8.18E-05	0.250561
CTSB	Cathepsin B	3	2.03E-04	0.271369
DDC	Aromatic-l-amino-acid/l-tryptophan decarboxylase	3	4.50E-04	0.225592
DGCR8	DGCR8, microprocessor complex subunit	3	2.59E-04	0.284
DYSF	Dysferlin	3	0	0.292181
FBL	rRNA 2'-O-methyltransferase fibrillarin	3	0	0.300269
GDF11	Growth/differentiation factor 11	3	1.21E-04	0.299693
GLS	Glutaminase kidney isoform, mitochondrial	3	3.57E-04	0.226969
GRN	Granulin precursor	3	0.001773	0.289045
GTF2H1	General transcription factor IIH subunit 1	3	7.18E-04	0.268201
HAVCR2	Hepatitis A virus cellular receptor 2	3	4.92E-05	0.266462
HBA1	Hemoglobin subunit alpha	3	0	0.260594
IFNA1	Interferon alpha-1/13	3	1.08E-05	0.270992
IHH	Indian hedgehog protein	3	0	0.271275
IL22	Interleukin-22	3	4.37E-05	0.266008
INHBA	Inhibin beta A chain	3	0	0.264119
ITPR1	Inositol 1,4,5-trisphosphate receptor type 1	3	3.92E-05	0.265466
KRT18	Keratin, type I cytoskeletal 18	3	4.83E-05	0.236667
LAMB2	Laminin subunit beta-2	3	1.64E-04	0.271558
LATS2	Serine/threonine-protein kinase LATS2	3	6.05E-04	0.235809
LMNB2	Lamin-B2	3	1.09E-04	0.295833
MC4R	Melanocortin receptor 4	3	0	0.247074
MIF	Macrophage migration inhibitory factor	3	7.90E-04	0.217246
MLKL	Mixed lineage kinase domain-like protein	3	0.002587	0.243986
MT-ND6	NADH-ubiquinone oxidoreductase chain 6	3	2.42E-05	0.287449
NDUFB3	NADH dehydrogenase [ubiquinone] 1 beta subcomplex subunit 3	3	8.09E-04	0.267741
NOX4	NADPH oxidase 4	3	1.16E-04	0.284517
NQO1	NAD(P)H dehydrogenase [quinone] 1	3	0.003238	0.295833
NRF1	Nuclear respiratory factor 1	3	0.002561	0.239277
NRP1	Neuropilin-1	3	7.14E-05	0.279328
OLR1	Oxidized low-density lipoprotein receptor 1	3	1.07E-05	0.253736
OSMR	Oncostatin-M-specific receptor subunit beta	3	6.38E-05	0.28629
PCK2	Phosphoenolpyruvate carboxykinase [GTP], mitochondrial	3	0.8	0.714286
PDGFC	Platelet-derived growth factor C	3	0	0.288511
PER2	Period circadian protein homolog 2	3	3.78E-05	0.294384
PPARGC1B	Peroxisome proliferator-activated receptor gamma coactivator 1-beta	3	0.005115	0.266099
PRDX5	Peroxiredoxin-5, mitochondrial	3	1.81E-04	0.296845
PRSS3P2	Trypsin-2	3	0	0.222191
PTPRA	Receptor-type tyrosine-protein phosphatase alpha	3	0.00105	0.278431
RBP4	Retinol-binding protein 4	3	0	0.275194
RDH5	11-cis retinol dehydrogenase	3	1.01E-04	0.28431
RDX	Radixin	3	1.14E-04	0.299808
RSPO3	R-spondin-3	3	0.002562	0.261029
SERPINB2	Plasminogen activator inhibitor 2	3	2.96E-05	0.278035
SF3B1	Splicing factor 3B subunit 1	3	2.24E-06	0.302011
SHMT1	Serine hydroxymethyltransferase, cytosolic	3	5.20E-06	0.282153
SLC40A1	Solute carrier family 40 member 1	3	2.63E-05	0.278431
SOST	Sclerostin	3	3.81E-05	0.274228
SRSF3	Serine/arginine-rich splicing factor 3	3	1.30E-04	0.262081
Continued				

Name	Name of protein	Degree	Betweenness centrality	Closeness centrality
ST3GAL4	CMP-N-acetylneuraminate-beta-galactosamide-alpha-2,3-sialyltransferase 4	3	1.95E-04	0.278829
STAM	Signal transducing adapter molecule 1	3	1.65E-04	0.256318
TFR2	Transferrin receptor protein 2	3	2.30E-05	0.232787
TLR5	Toll-like receptor 5	3	1.09E-06	0.232787
TMEM173	Stimulator of interferon genes protein	3	0	0.286816
TNFRSF4	Tumor necrosis factor receptor superfamily member 4	3	8.34E-05	0.271275
TREM1	Triggering receptor expressed on myeloid cells 1	3	6.58E-05	0.27471
TRIM33	E3 ubiquitin-protein ligase TRIM33	3	0	0.256992
ACE	Angiotensin-converting enzyme	2	3.13E-05	0.298319
ACER3	Alkaline ceramidase 3	2	8.06E-04	0.257671
ACTC1	Actin, alpha cardiac muscle 1	2	0	0.214502
ADD1	Alpha-adducin	2	0	0.264656
ADIPOR1	Adiponectin receptor protein 1	2	0	0.243454
ADIPOR2	Adiponectin receptor protein 2	2	3.76E-05	0.266644
AKR1A1	Alcohol dehydrogenase [NADP(+)]	2	1.28E-05	0.295386
AKR1B1	Aldose reductase	2	4.50E-06	0.24391
AKR1B10	Aldo-keto reductase family 1 member B10	2	1.47E-05	0.2726
ALDH1B1	Aldehyde dehydrogenase 1 family member b1	2	0	0.257246
ANXA6	Annexin A6	2	0	0.257246
AVP	Vasopressin-neurophysin 2-copeptin	2	2.48E-05	0.26314
B3GAT1	Galactosylgalactosylxylosylprotein 3-beta-glucuronosyltransferase 1	2	3.60E-06	0.301894
CCRL2	C-C chemokine receptor-like 2	2	6.35E-05	0.207823
CES2	Cocaine esterase	2	2.47E-04	0.220621
CTBP2	C-terminal-binding protein 2	2	0	0.220124
DICER1	Dicer 1, ribonuclease iii	2	0	0.220124
EIF6	Eukaryotic translation initiation factor 6	2	6.28E-05	0.267833
FFAR1	Free fatty acid receptor 1	2	1.16E-04	0.298092
FPR2	Formyl peptide receptor-like	2	1.89E-05	0.246917
FTH1	Ferritin heavy chain	2	4.19E-05	0.243606
GDF2	Growth/differentiation factor 2	2	4.65E-04	0.271936
GGT1	Glutathione hydrolase 1 proenzyme	2	8.23E-05	0.207437
GNMT	Glycine N-methyltransferase	2	0.003247	0.2726
GPNMB	Transmembrane glycoprotein NMB	2	5.08E-05	0.288938
GPR119	Glucose-dependent insulinotropic receptor	2	0	0.25218
GREM1	Gremlin-1	2	0	0.25218
GSDMD	Gasdermin-D	2	0	0.29383
HBB	Hemoglobin subunit beta	2	0	0.243378
HCFC1	Host cell factor 1	2	0.005115	0.238255
HMMR	Hyaluronan mediated motility receptor	2	0.002561	0.192554
HNRNPU	Heterogeneous nuclear ribonucleoprotein U	2	4.75E-05	0.283176
HSPA12A	Heat shock protein family A member 12 A	2	6.52E-05	0.213446
IL11	Interleukin-11	2	4.43E-05	0.271463
IL13RA2	Interleukin-13 receptor subunit alpha-2	2	0.002561	0.251935
KLF6	Krueppel-like factor 6	2	0	0.309798
LGALS3BP	Galectin-3-binding protein	2	0	0.300269
LMF1	Lipase maturation factor 1	2	1.22E-05	0.198073
LPCAT3	Lysophospholipid acyltransferase 5	2	7.00E-04	0.228764
LRPAP1	Alpha-2-macroglobulin receptor-associated protein	2	1.73E-05	0.198778
MKL1	MKL/myocardin-like protein 1	2	0.4	0.555556
MOCOS	Molybdenum cofactor sulfurase	2	0	0.295163
MYOM2	Myomesin-2	2	2.33E-04	0.284725
NCAN	Neurocan core protein	2	0	0.297184
NLRC3	NLR family CARD domain-containing protein 3	2	0	0.23913
NRG4	Pro-neuregulin-4, membrane-bound isoform	2	0.002561	0.208879
P2RX7	P2X purinoceptor 7	2	0	0.274035
PEMT	Phosphatidylethanolamine N-methyltransferase	2	0.002561	0.190907
Continued				

Name	Name of protein	Degree	Betweenness centrality	Closeness centrality
PLIN5	Perilipin-5	2	0	0.24202
POSTN	Periostin	2	0	0.215985
PRPF8	Pre-mRNA-processing-splicing factor 8	2	1.37E-06	0.221938
PSPH	Phosphoserine phosphatase	2	0	0.242321
RARRES2	Retinoic acid receptor responder protein 2	2	0	0.238182
SALL4	Sal-like protein 4	2	1.37E-04	0.272315
SART1	U4/U6.U5 tri-snRNP-associated protein 1	2	0	0.310044
SDF2L1	Stromal cell-derived factor 2-like protein 1	2	0	0.264387
SHBG	Sex hormone-binding globulin	2	6.60E-07	0.25657
SLC10A1	Solute carrier family 10 (sodium/bile acid cotransporter), member 1	2	0	0.268754
SLC11A2	Natural resistance-associated macrophage protein 2	2	0	0.302596
SLC2A1	Solute carrier family 2, facilitated glucose transporter member 1	2	1.52E-04	0.218829
SLPI	Secretory leukocyte peptidase inhibitor	2	5.22E-05	0.216164
SOCS7	Suppressor of cytokine signaling 7	2	2.20E-05	0.259296
SPINK1	Serine protease inhibitor Kazal-type 1	2	0.002561	0.295274
STK25	Serine/threonine-protein kinase 24/25/mst4	2	4.86E-05	0.275777
TCF4	Transcription factor 4	2	0.002561	0.242396
TF	Serotransferrin	2	0.4	0.555556
TGM2	Protein-glutamine gamma-glutamyltransferase 2	2	0	0.264746
TNFRSF12A	Tumor necrosis factor receptor superfamily member 12 A	2	0	0.210285
TRIM21	Tripartite motif-containing protein 21	2	0	0.210285
UBXN1	UBX domain-containing protein 1	2	0	0.274517
XDH	Xanthine dehydrogenase/oxidase	2	0	0.270898
ABCC3	Canalicular multispecific organic anion transporter 2	1	5.41E-05	0.195152
ARRDC3	Arrestin domain-containing protein 3	1	0	0.196626
ATP5E	ATP synthase subunit epsilon, mitochondrial	1	0	0.255982
ATP7B	Copper-transporting ATPase 2	1	0	0.262081
ATP8B1	Phospholipid-transporting ATPase IC	1	0	0.262169
BCAT1	Branched-chain-amino-acid aminotransferase, cytosolic	1	0	0.237314
BCAT2	Branched-chain-amino-acid aminotransferase, mitochondrial	1	0	0.237314
CD34	Hematopoietic progenitor cell antigen CD34	1	0	0.255982
CD82	CD82 antigen	1	0	0.255982
CHST2	Carbohydrate sulfotransferase 2	1	0	0.234183
CIDEA	Cell death inducing dffa like effector a	1	0	0.234183
CIDEB	Cell death inducing dffa like effector b	1	0	0.282766
CMKLR1	Chemokine-like receptor 1	1	0	0.267649
CNR2	Cannabinoid receptor 2	1	0	0.197422
CPA1	Carboxypeptidase A1	1	0	0.213797
CPN1	Carboxypeptidase N catalytic chain	1	0	0.209383
CRABP2	Cellular retinoic acid-binding protein 2	1	0	0.209383
CRELD2	Cysteine rich with EGF like domains 2	1	0	0.218706
CTCFL	Transcriptional repressor CTCFL	1	0	0.218706
CXCL16	C-X-C motif chemokine 16	1	0	0.215627
CXCL5	C-X-C motif chemokine 5	1	0	0.267741
CXCR5	C-X-C chemokine receptor type 5	1	0	0.282869
CXCR6	C-X-C chemokine receptor type 6	1	0	0.213039
DCTN4	Dynactin subunit 4	1	0	1
DECR1	2,4-dienoyl-CoA reductase, mitochondrial	1	0	1
DMGDH	Dimethylglycine dehydrogenase, mitochondrial	1	0	0.232164
ECHS1	Enoyl-CoA hydratase, mitochondrial	1	0	0.161497
EDA	Ectodysplasin-A	1	0	0.212923
EIF2AK1	Eukaryotic translation initiation factor 2-alpha kinase 1	1	0	0.212923
FABP2	Fatty acid-binding protein, intestinal	1	0	0.196182
FBXW5	F-box/WD repeat-containing protein 5	1	0	0.228096
FFAR4	Free fatty acid receptor 4	1	0	0.201289
FOXA3	Hepatocyte nuclear factor 3-gamma	1	0	1
Continued				

Name	Name of protein	Degree	Betweenness centrality	Closeness centrality
FTL	Ferritin light chain	1	0	1
GCGR	Glucagon receptor	1	0	1
GCKR	Glucokinase regulatory protein	1	0	1
GDF15	Growth differentiation factor 15	1	0	0.234043
GFER	Growth factor, augmenter of liver regeneration	1	0	0.254979
GOLM1	Golgi membrane protein 1	1	0	0.23244
GPBAR1	G-protein coupled bile acid receptor 1	1	0	0.246684
GPLD1	Glycosylphosphatidylinositol specific phospholipase d1	1	0	0.201133
GPR55	G protein-coupled receptor 55	1	0	0.270711
GSTA4	Glutathione S-transferase A4	1	0	0.384615
GSTM2	Glutathione S-transferase Mu 2	1	0	0.256234
HDAC8	Histone deacetylase 8	1	0	0.208156
HS3ST1	[heparan sulfate]-glucosamine 3-sulfotransferase 1	1	0	0.259124
HSPA6	Heat shock 70 kDa protein 6	1	0	0.228764
HTR2A	5-hydroxytryptamine receptor 2 A	1	0	0.23251
IBTK	Inhibitor of Bruton tyrosine kinase	1	0	0.289796
IFNA13	Interferon alpha-1/13	1	0	0.259382
IGFBP2	Insulin-like growth factor-binding protein 2	1	0	0.252587
IL19	Interleukin-19	1	0	1
IL20RA	Interleukin-20 receptor subunit alpha	1	0	1
IL33	Interleukin-33	1	0	0.172826
INTU	Protein inturned	1	0	0.25316
ITPR2	Inositol 1,4,5-trisphosphate receptor type 2	1	0	0.283691
KRT19	Keratin, type I cytoskeletal 19	1	0	0.160337
LIN28B	Protein lin-28 homolog B	1	0	0.241796
LIPA	Lysosomal acid lipase/cholesteryl ester hydrolase	1	0	0.235454
LTBP3	Latent-transforming growth factor beta-binding protein 3	1	0	0.249361
MBOAT7	Membrane bound o-acyltransferase domain containing 7	1	0	0.23717
MDK	Midkine	1	0	0.242848
MERTK	Tyrosine-protein kinase Mer	1	0	0.220809
MGAM	Maltase-glucoamylase, intestinal	1	0	0.220809
MMP11	Matrix metalloproteinase-11 (stromelysin 3)	1	0	0.267741
MTHFR	Methylenetetrahydrofolate reductase (nadph)	1	0	0.252098
NFE2L1	Nuclear factor erythroid 2-related factor 1	1	0	0.251773
NOX1	NADPH oxidase 1	1	0	0.235454
NPPB	Natriuretic peptides B	1	0	1
NTS	Neurotensin/neuromedin N	1	0	1
ORM1	Alpha-1-acid glycoprotein 1	1	0	0.262698
PANX1	Pannexin-1	1	0	0.207052
PDE4A	cAMP-specific 3',5'-cyclic phosphodiesterase 4 A	1	0	0.264119
PHGDH	D-3-phosphoglycerate dehydrogenase	1	0	1
PRMT7	Protein arginine N-methyltransferase 7	1	0	1
RAG2	V(D)J recombination-activating protein 2	1	0	0.248805
RASSF1	Ras association domain-containing protein 1	1	0	0.239277
SAMM50	Sorting and assembly machinery component 50 homolog	1	0	0.217913
SERPINA12	Serpin A12	1	0	0.267741
SESN3	Sestrin 1/3	1	0	0.240086
SFRP4	Secreted frizzled-related protein 4	1	0	0.282869
SFRP5	Secreted frizzled-related protein 5	1	0	0.248726
SH3BP5	SH3 domain-binding protein 5	1	0	1
SI	Sucrase-isomaltase, intestinal	1	0	1
SLAMF1	Signaling lymphocytic activation molecule	1	0	0.27695
SLC51A	Organic solute transporter subunit alpha	1	0	0.215746
SLC5A2	Sodium/glucose cotransporter 2	1	0	0.228029
SLC6A3	Solute carrier family 6 (neurotransmitter transporter, dopamine) member 3	1	0	0.268754
SLC6A4	Sodium-dependent serotonin transporter	1	0	1
Continued				

Name	Name of protein	Degree	Betweenness centrality	Closeness centrality
SLCO1A2	Solute carrier organic anion transporter family member 1A2	1	0	1
SRSF6	Splicing factor, arginine/serine-rich 4/5/6	1	0	0.250642
STAR	Steroidogenic acute regulatory protein, mitochondrial	1	0	0.454545
TM6SF2	Transmembrane 6 superfamily member 2	1	0	0.265195
TMBIM6	Bax inhibitor 1	1	0	0.23717
TMED2	Transmembrane emp24 domain-containing protein 2	1	0	0.195152
TMSB4X	Thymosin beta 4, x-linked	1	0	0.384615
TNC	Tenascin	1	0	0.210342
TNFRSF6B	Tumor necrosis factor receptor superfamily, member 6b, decoy	1	0	0.21527
TNIP3	TNFAIP3-interacting protein 3	1	0	0.279328
TRPC4AP	Short transient receptor potential channel 4-associated protein	1	0	0.247937
TUBA8	Tubulin alpha-8 chain	1	0	0.276656
UBQLN4	Ubiquilin-4	1	0	0.230997
UCP1	Mitochondrial brown fat uncoupling protein 1	1	0	0.295051
UFM1	Ubiquitin-fold modifier 1	1	0	0.244674
UFSP2	Ufm1-specific protease 2	1	0	0.23753
VSIG4	V-set and immunoglobulin domain-containing protein 4	1	0	0.262698
WDR1	WD repeat-containing protein 1	1	0	0.245366
WTAP	Pre-mRNA-splicing regulator WTAP	1	0	0.193126
ZCCHC11	Zinc finger cchc-type containing 11	1	0	0.24202
ZNF638	Zinc finger protein 638	1	0	1

Table 1. Basic information on NASH disease targets in the protein interaction network map.

proteins are shown in Table 7 and the 3-dimensional map of the binding sites is shown in Fig. 6. The docking results demonstrate that diosgenin is capable of forming hydrogen bonds with these proteins, with bond lengths significantly shorter than the conventional 3.5 Å associated with standard hydrogen bonds. The binding energies are all below −7 kcal/mol, which confirms a relatively strong binding ability and suggests potential interactions among them.

Assessment of HepG2 cell viability and morphology under FFA and diosgenin treatment

Since the signaling pathway with the most enriched targets in the KEGG enrichment analysis was the PI3K-Akt pathway, and all of the nine core targets (ALB[45], AKT1, TP53[46], VEGFA[47], MAPK3[48], EGFR[49], STAT3[50], CASP3[44], IGF1[51]) were related to the PI3K-Akt pathway, we thus hypothesized that diosgenin affects NASH by alleviating triglyceride deposition and the inflammatory response through the PI3K-Akt pathway. To confirm this hypothesis, HepG2 cells were treated with free fatty acids (FFAs) at a 1:2 molar ratio of palmitic acid (PA) to oleic acid (OA), aiming to simulate NASH in *vitro*[52]. Initially, the effective concentrations of both FFA and diosgenin were determined using the CCK-8 assay. The FFA concentration gradient ranged from 0.1 to 0.5 mM. The findings demonstrated that the viability of HepG2 cells was significantly inhibited when the concentration of PA in the FFA solution exceeded 0.1 mM (Fig. 7A). The highest concentration surpassing the median lethal dose (LD50), namely, the FFA containing 0.2 mM PA, was chosen for the subsequent experiments. Subsequently, HepG2 cells were treated with different concentrations of diosgenin at 0, 5, 10, 25, 50, and 100 μM. Figure 7B shows that there was no significant effect on cell viability at diosgenin concentrations ranging from 0 to 25 μM. However, cell viability was dramatically inhibited when the concentration of diosgenin was greater than 25 μM. Therefore, 5, 10, and 25 μM diosgenin were used in the following experiments. The morphology of the HepG2 cells in the various groups is depicted in Fig. 7C. The cell number decreased, and the cell morphology changed after 24 h of FFA treatment. The cell condition improved after 5 μM diosgenin treatment and was further enhanced in the 10 μM treatment group. However, 25 μM diosgenin treatment did not ameliorate these changes.

Diosgenin alleviates triglyceride deposition and the inflammatory response in FFA-treated HepG2 cells

To verify the effects of diosgenin on lipid metabolism in hepatocytes, we measured the intracellular TG, TC and FC levels in diosgenin-treated HepG2 cells. The intracellular TG content was significantly greater in the FFA-treated group than in the control group. Additionally, the intracellular TG content tended to decrease after 5 μM diosgenin treatment and further decreased after 10 μM diosgenin treatment (Fig. 8B). However, the concentration of 25 μM diosgenin did not significantly affect the lowering of TG levels. Consistent with these findings, Oil Red O staining (Fig. 8A) revealed that the intracellular lipid content was significantly greater in HepG2 cells after 24 h of FFA treatment than in normal controls, and the lipid content was reduced by the addition of 5 μM diosgenin. The intracellular lipid droplet content was significantly reduced after 10 μM diosgenin treatment. Although FFA treatment for 24 h did not increase cholesterol levels in the NASH cell model, treatment with 10 μM diosgenin for 24 h resulted in notable decreases in total cholesterol (TC) and total fibrin (FC) levels in the cells (Fig. 8C).

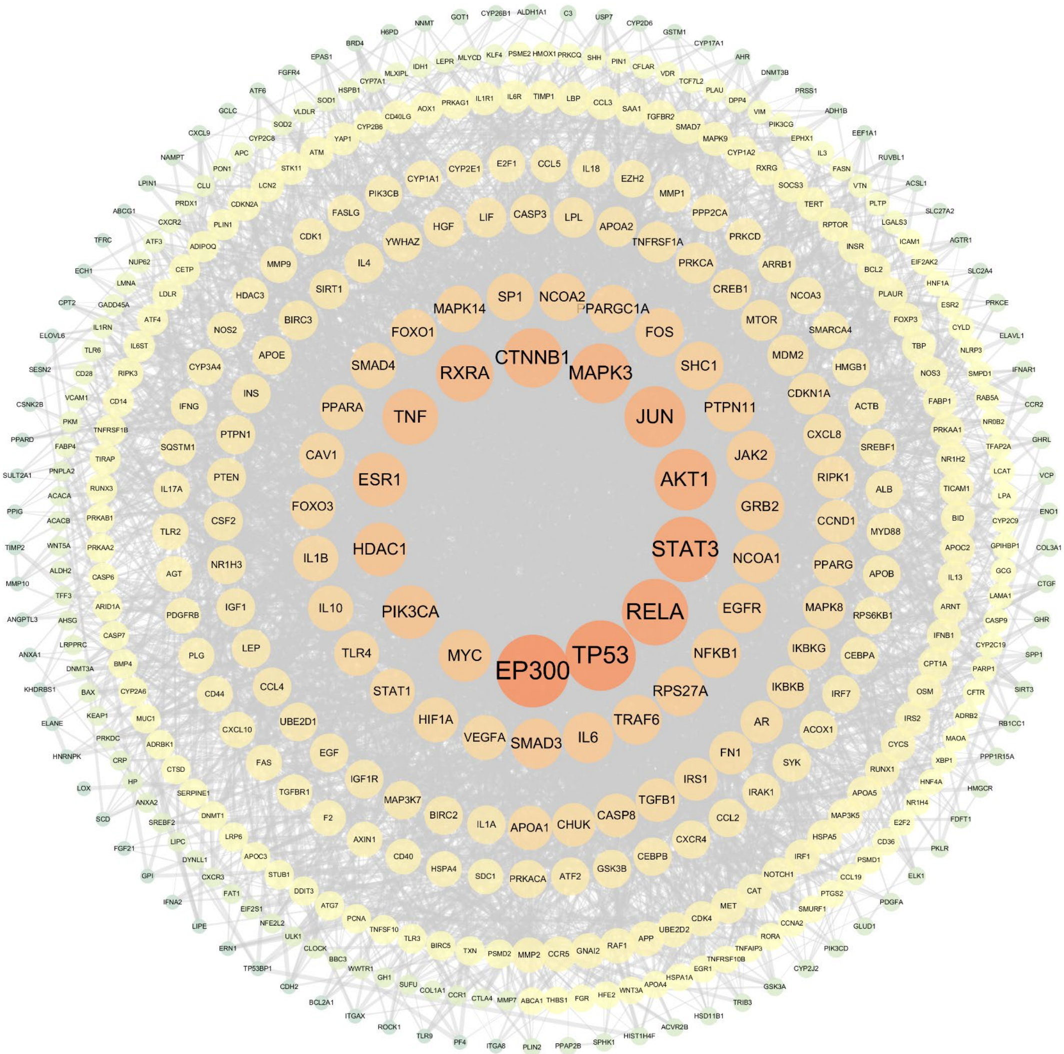

Fig. 3. PPI network map of nonalcoholic steatohepatitis (NASH)-related targets. The size and color of the nodes. Are sorted in descending order by degree value from largest to smallest and from red to yellow. The figure displays targets with a degree of 9 or higher.

To assess the ameliorative effect of diosgenin on NASH-related inflammation, we also measured the inflammatory factor IL-6 in the culture supernatant of a diosgenin-treated NASH cell model using an enzyme-linked immunosorbent assay. The IL-6 concentration in the culture supernatant of FFA-treated cells was elevated nearly 1.5-fold compared with that in the normal control group, and treatment with diosgenin significantly reduced the elevated IL-6 level (Fig. 8D).

Diosgenin ameliorates triglyceride deposition and inflammation through the PI3K-Akt pathway in FFA-treated HepG2 cells

The results of the network pharmacological analysis showed that diosgenin might attenuate fatty acid metabolism through the PI3K-Akt pathway in NASH therapy. To further verify whether diosgenin activates the PI3K-Akt pathway and thus plays a role in the treatment of NASH, we examined the protein expression levels of PI3K, p-AKT, and AKT by western blotting. These findings indicate that the phosphorylation level of AKT decreased by approximately 32.7% in HepG2 cells treated with FFA, while diosgenin significantly enhanced the phosphorylation of AKT. However, there was no significant change in the phosphorylation of PI3K between the groups (Fig. 9A, B). We observed that the protein expression of stearoyl-coenzyme A desaturase-1 (SCD1), which is closely related to fatty acid synthesis, was increased in the NASH cell line, and its expression was significantly decreased after treatment with 10 μM diosgenin (Fig. 8E, F). However, there was no significant difference in the expression of other key proteins involved in fatty acid metabolism, such as FASN, ACC, p-ACC, SREBP1c and CPT1α (Fig. 9C–F).

Name	Name of protein	Degree	Betweenness centrality	Closeness centrality
ALB	RAC-alpha serine/threonine-protein kinase	80	0.105112	0.78169
AKT1	Aldose reductase	72	0.051785	0.74
TP53	Cellular tumor antigen p53	66	0.03787	0.711538
VEGFA	Vascular endothelial growth factor A	64	0.028961	0.698113
MAPK3	Mitogen-activated protein kinase 3	62	0.040054	0.689441
EGFR	Epidermal growth factor receptor	59	0.029649	0.680982
STAT3	Signal transducer and activator of transcription 3	59	0.04422	0.680982
CASP3	Branched-chain-amino-acid aminotransferase, mitochondrial	58	0.018328	0.668675
IGF1	Insulin-like growth factor I	57	0.026075	0.668675
PPARG	Peroxisome proliferator-activated receptor gamma	56	0.038014	0.660714
ESR1	Estrogen receptor	55	0.022216	0.664671
MTOR	Serine/threonine-protein kinase mTOR	50	0.0163	0.641619
MMP9	Matrix metalloproteinase-9	49	0.017083	0.634286
PPARA	Peroxisome proliferator-activated receptor alpha	49	0.041892	0.634286
CCND1	G1/S-specific cyclin-D1	48	0.013186	0.634286
HIF1A	Hypoxia-inducible factor 1-alpha	48	0.011672	0.630682
CAT	Caspase-7	47	0.042191	0.634286
PTGS2	Prostaglandin G/H synthase 2	46	0.010637	0.627119
MAPK14	Mitogen-activated protein kinase 14	42	0.010223	0.61326
RELA	Rela proto-oncogene, nf-kb subunit	40	0.010737	0.6
MAPK8	Mitogen-activated protein kinase 8/9/10 (c-jun n-terminal kinase)	39	0.005198	0.603261
NOS3	Nitric-oxide synthase, endothelial	39	0.006608	0.6
MMP2	Matrix metalloproteinase-2 (gelatinase a)	38	0.005338	0.596774
CYP3A4	Cytochrome p450 family 3 subfamily a polypeptide 4	37	0.028431	0.587302
IGF1R	Insulin-like growth factor 1 receptor	37	0.003095	0.596774
MDM2	E3 ubiquitin-protein ligase Mdm2	37	0.005473	0.587302
STAT1	Signal transducer and activator of transcription 1-alpha/beta	37	0.007163	0.587302
GSK3B	Glycogen synthase kinase-3 beta	36	0.002792	0.590426
HMOX1	Heme oxygenase 1	36	0.006587	0.593583
AR	Amyloid-beta A4 protein	34	0.005159	0.584211
CDKN1A	Cyclin-dependent kinase inhibitor 1	34	0.001527	0.57513
ICAM1	Intercellular adhesion molecule 1	34	0.004929	0.584211
JAK2	Tyrosine-protein kinase JAK2	34	0.004738	0.57513
APP	Apolipoprotein A-II	33	0.005819	0.581152
SOD2	Superoxide dismutase [Mn], mitochondrial	33	0.016237	0.584211
GRB2	Growth factor receptor-bound protein 2	31	0.021606	0.569231
PTPN11	Tyrosine-protein phosphatase nonreceptor type 11	31	0.004814	0.572165
PARP1	Poly [ADP-ribose] polymerase 1	29	0.009258	0.563452
GSTP1	Glutathione S-transferase P	28	0.017789	0.566327
PDGFRB	Platelet-derived growth factor receptor beta	28	0.0026	0.555
CDK4	Cyclin-dependent kinase 4	27	8.19E-04	0.549505
MET	Hepatocyte growth factor receptor	26	9.08E-04	0.541463
ESR2	Estrogen receptor beta	25	0.002895	0.544118
PTPN1	Tyrosine-protein phosphatase nonreceptor type 1	25	0.001351	0.555
RXRA	Retinoic acid receptor RXR-alpha	25	0.015233	0.538835
CYP19A1	Aromatase	24	0.004316	0.546798
FASN	Fatty acid synthase	24	0.006278	0.546798
SOD1	Superoxide dismutase, cu-zn family	24	0.003079	0.552239
CYP2C9	Cytochrome p450 family 2 subfamily c polypeptide 9	22	0.006526	0.528571
SHH	Sonic hedgehog protein	22	6.34E-04	0.528571
AKR1B1	Adenosine A2a receptor	21	0.004587	0.538835
CDK1	Cyclin-dependent kinase 1	21	8.05E-04	0.541463
F2	Prothrombin	21	0.005701	0.536232
GSR	Glutathione reductase, mitochondrial	21	0.002246	0.541463
NQO1	NAD(P)H dehydrogenase [quinone] 1	21	0.001801	0.536232
INSR	Insulin receptor	20	0.001153	0.528571
Continued				

Name	Name of protein	Degree	Betweenness centrality	Closeness centrality
CASP7	Caspase-3	18	1.37E-04	0.521127
CTSB	Cathepsin B	18	0.001531	0.526066
GSTA1	Glutathione S-transferase A1	18	0.00511	0.506849
GSTM1	Glutathione S-transferase Mu 1	18	0.005783	0.518692
NR1H4	Bile acid receptor	18	0.004847	0.533654
SERPINA1	Alpha-1-antitrypsin	18	0.003425	0.513889
TNFRSF10B	Tumor necrosis factor receptor superfamily member 10B	18	5.97E-04	0.528571
DPP4	Dipeptidyl peptidase 4	17	0.001433	0.526066
PLA2G4A	Cytosolic phospholipase A2	17	0.003383	0.523585
TGFBR1	TGF-beta receptor type-1	17	3.31E-04	0.511521
PIK3CG	Phosphatidylinositol 4,5-bisphosphate 3-kinase catalytic subunit gamma isoform	16	7.31E-04	0.497758
SYK	Spleen associated tyrosine kinase	16	0.001011	0.523585
ABCC2	Atp-binding cassette, subfamily c (cftr/mrp), member 2	15	0.003047	0.495536
CYP2C8	Cytochrome p450 family 2 subfamily c polypeptide 8	15	0.001822	0.506849
VDR	Vitamin D3 receptor	15	3.79E-04	0.521127
HMGCR	3-hydroxy-3-methylglutaryl-coenzyme A reductase	14	0.001999	0.506849
LCN2	Neutrophil gelatinase-associated lipocalin	14	0.001538	0.506849
MAPK9	Mitogen-activated protein kinase 8/9/10 (c-jun n-terminal kinase)	14	3.88E-04	0.495536
MMP13	Matrix metalloproteinase-13 (collagenase 3)	14	1.02E-04	0.513889
NR1I2	Nuclear receptor subfamily 1 group I member 2	14	0.002824	0.516279
PRKACA	cAMP-dependent protein kinase catalytic subunit alpha	14	0.001497	0.5
SULT2A1	Sulfotransferase family 2a member 1	14	0.001889	0.480519
FGFR4	Fibroblast growth factor receptor 4	13	6.35E-04	0.502262
GSTM2	Glutathione S-transferase Mu 2	13	0.002412	0.488987
RAB5A	RAB5A, member RAS oncogene family	13	4.01E-04	0.506849
CYP17A1	Steroid 17-alpha-hydroxylase/17,20 lyase	12	0.001418	0.474359
ELANE	Elastase, neutrophil expressed	12	7.61E-04	0.486842
TTR	Transthyretin	12	0.002221	0.493333
NR1H3	Oxysterols receptor LXR-alpha	11	9.67E-04	0.478448
PPARD	Peroxisome proliferator-activated receptor delta	11	0.001725	0.478448
RBP4	Retinol-binding protein 4	11	0.001501	0.49115
APOA2	Aldehyde dehydrogenase, mitochondrial	10	0.001051	0.493333
FGR	Fgr proto-oncogene, src family tyrosine kinase	10	0.001463	0.460581
CCR1	C-C chemokine receptor type 1	9	4.63E-04	0.449393
CES1	Liver carboxylesterase 1	9	6.94E-04	0.482609
SHBG	Sex hormone-binding globulin	9	6.58E-04	0.476395
ALDH2	Serum albumin	8	0.001158	0.418868
HSD11B1	Corticosteroid 11-beta-dehydrogenase isozyme 1	8	3.41E-04	0.480519
NR1H2	Oxysterols receptor LXR-beta	8	2.96E-04	0.440476
NR1I3	Nuclear receptor subfamily 1 group I member 3	8	5.13E-04	0.478448
PRKCQ	Protein kinase C theta type	8	6.05E-05	0.458678
NPC1L1	Niemann-Pick C1-like protein 1	7	7.58E-04	0.464435
S100A9	Protein S100-A9	7	4.28E-04	0.435294
THRB	Thyroid hormone receptor beta	7	0.001281	0.478448
ACADM	Abo, alpha 1-3-n-acetylgalactosaminyltransferase and alpha 1-3-galactosyltransferase	6	6.45E-04	0.458678
ADH1C	Medium-chain specific acyl-CoA dehydrogenase, mitochondrial	6	2.90E-04	0.376271
ADORA2A	Alcohol dehydrogenase 1c (class i), gamma polypeptide	6	0	0.478448
BCAT2	Androgen receptor	6	0.001248	0.430233
IL6ST	Interleukin-6 receptor subunit beta	6	0	0.444
MAOA	Amine oxidase [flavin-containing] A	5	8.13E-04	0.428571
CRABP2	Chitotriosidase-1	4	1.44E-04	0.437008
Continued				

Name	Name of protein	Degree	Betweenness centrality	Closeness centrality
HTR2A	5-hydroxytryptamine receptor 2 A	4	2.91E-04	0.460581
HDAC8	Histone deacetylase 8	3	3.27E-05	0.433594
RORA	Rar-related orphan receptor alpha	3	0	0.422053
YARS	Tyrosine–tRNA ligase, cytoplasmic	3	1.07E-04	0.393617
MERTK	Tyrosine-protein kinase Mer	1	0	0.363934

Table 2. Topological information on the diosgenin and NASH targets.

Discussion

In this study, we investigated the potential role that diosgenin plays in NASH remission. Network pharmacology was employed to predict the candidate therapeutic targets and signaling pathways of diosgenin in NASH, and then, experimental verification in HepG2 cells was conducted to further illustrate the pharmacological mechanism of diosgenin against NASH.

Based on the results of the PPI network topology analysis, 9 key genes related to the association of diosgenin with NASH were screened, the most important of which was AKT1. The protein kinase AKT is a serine threonine protein kinase that is activated in response to different stimuli through a phosphatidylinositol 3 kinase (PI3K)-dependent mechanism[53] and plays a central role in promoting cell proliferation, migration and transcription and inhibiting apoptosis. Akt1 is a subtype of the Akt family[54,55]. Each Akt isoform plays a different role in metabolism and growth processes. However, Akt1 plays a key role in cell growth and survival[56,57]. In addition, several studies have shown that AKT plays an important role in the regulation of lipid metabolism. The results of KEGG pathway analysis showed that the signaling pathway with the most enriched targets was the PI3K-Akt pathway (hsa04151). The PI3K-Akt signaling pathway functions in organism growth and key cellular processes such as glucose homeostasis, lipid metabolism, protein synthesis, cell proliferation and survival by mediating growth factor signaling[58]. Several studies have shown that the PI3K-Akt pathway plays an important role in regulating lipid metabolism. Brg1 regulates lipid metabolism in hepatocellular carcinoma by mediating GLMP expression through the PIK3AP1/PI3K/AKT pathway[59]. LAMP3 regulates hepatic lipid metabolism through activation of the PI3K/Akt pathway[60]. Scutellaria baicalensis and Radix Scutellariae improve glycolipid metabolism in T2DM rats by modulating the metabolic profile and the MAPK/PI3K/Akt signaling pathway[61]. In addition, the PI3K-Akt pathway plays a crucial role in the development of inflammation. The PTX3/TIST1 feedback loop regulates lipopolysaccharide-induced inflammation via the PI3K/Akt signaling pathway[62]. Moreover, macrolides reduce pulmonary and systemic inflammation in COPD by modulating the PI3K/Akt-Nrf2 pathway[63]. Our experimental results suggest that diosgenin may ameliorate steatosis and attenuate the inflammatory response in HepG2 cells by activating the PI3K-Akt pathway.

Other core genes are discussed below. ALB is a carrier of fatty acids in the blood. It has been found that defective phosphorylation of TP53 at Ser312 leads to disruption of lipid metabolism, which causes fat accumulation and even the development of fatty liver[64]. Hepatocyte-derived VEGFA accelerates the progression of NAFLD to hepatocellular carcinoma through the activation of hepatic stellate cells[65]. MAPK3, or ERK1, plays key roles in many cell proliferation-related signaling pathways. EGFR is closely related to lipid rafts and plays an important role in the development of tumorigenesis[66]. Overexpression of STAT3 in the liver ameliorated hyperglycemia and hyperinsulinemia in insulin-resistant diabetic mice[67]. The protein encoded by the CASP3 gene is a cysteine-aspartate protease that plays a key role in the execution phase of apoptosis, and inhibition of CASP3 can reduce hepatocyte apoptosis and attenuate alcohol-induced liver injury[68]. It has been shown that IGF1 inhibits cholesterol accumulation in the liver of growth hormone-deficient mice through activation of ABCA1[69]. The above proteins play important roles in the liver and are likely to play an equal role in the development of NASH; moreover, whether diosgenin exerts effects on NASH through these key targets needs to be further confirmed.

In recent years, diosgenin has received increasing attention for its efficacy in the treatment of various metabolic diseases and has been used to treat various cancers[70], atherosclerosis[71], skin diseases[72], osteoporosis[73], neurological diseases[74], and metabolic diseases (obesity, diabetes, inflammation)[75]. It has been reported that diosgenin upregulates the expression of the caveolin-1 protein, which is closely related to cholesterol transport, and reduces intracellular cholesterol levels in human normal hepatocyte L02 cells[76]. In the present study, we investigated the triglyceride-lowering effect of diosgenin in a NASH cell model. Moreover, our experiments confirmed that diosgenin treatment significantly reduced intracellular cholesterol levels, which is consistent with the findings of the previous studies mentioned above.

Fatty acid synthesis is an important process in lipid metabolism. Stearoyl coenzyme A desaturase 1 (SCD1) is the rate-limiting enzyme in the biosynthesis of monounsaturated fatty acids[77]. Both systemic SCD1 knockout mice and liver-specific SCD1 knockout mice exhibit decreased hepatic triglyceride accumulation and resistance to high-fat diet (HFD)- or high-carbohydrate diet-induced steatosis[78–80]. Our experimental results suggest that diosgenin can reduce SCD1 protein expression in HepG2 cells and ameliorate hepatic lipids by reducing lipid synthesis. It is known that inflammatory cytokines play a key role in the pathogenesis and progression of NASH, leading to more severe fatty liver conditions[81]. It has been demonstrated that diosgenin can reduce proinflammatory and prosurvival signaling in cancer cells[82]. Our results showed that diosgenin significantly alleviated IL-6 secretion in a NASH cell model. These in *vitro* studies confirm diosgenin's dual therapeutic effects: improving hepatocyte lipid metabolism and reducing inflammation in NASH.

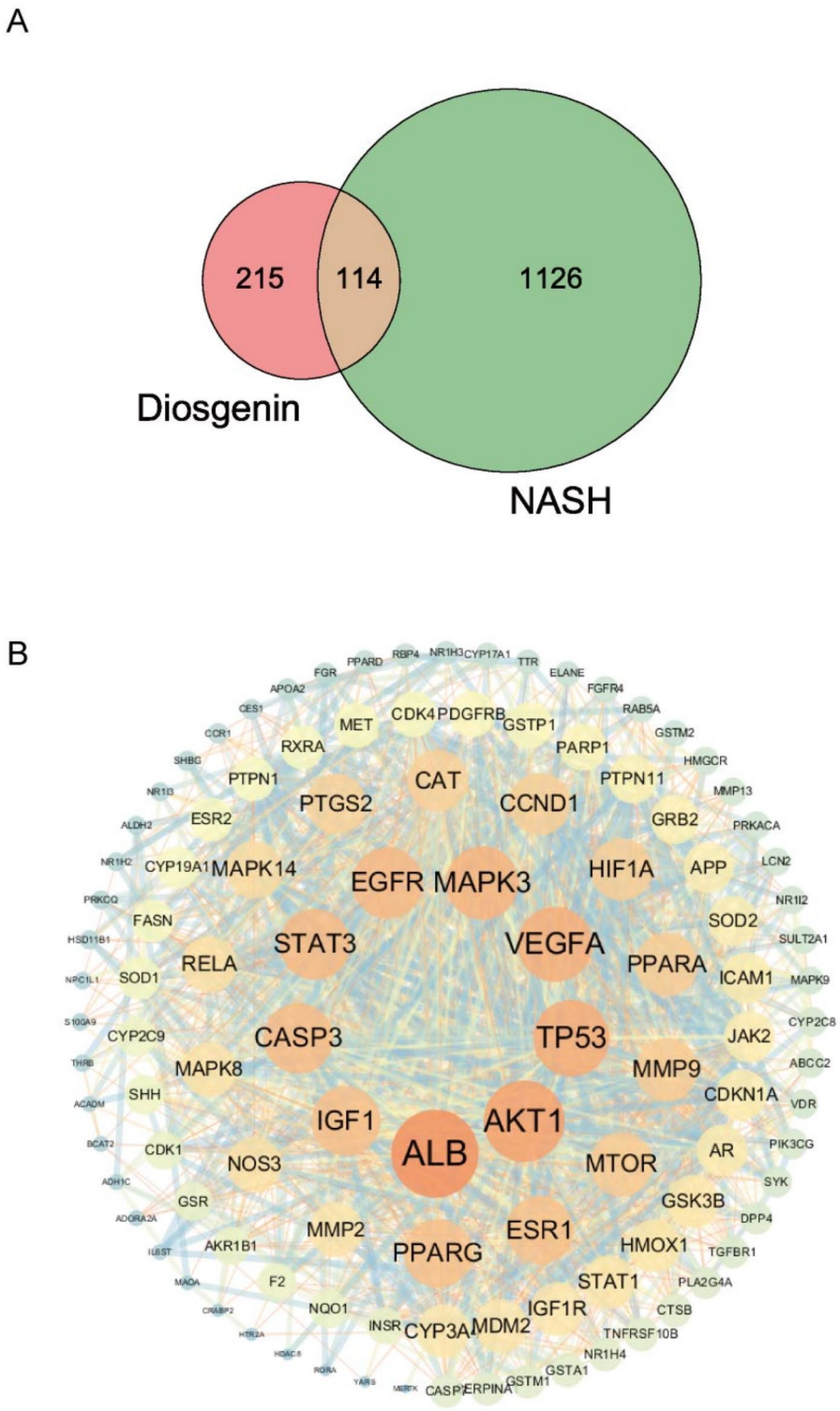

Fig. 4. Target screening of the effect of diosgenin on NASH. (**A**) Venn diagram of Diosgenin and NASH targets; (**B**) PPI network of Diosgenin and NASH intersection targets. The targets are sorted incrementally by degree-value, and the node colors and sizes are adjusted according to the degree values. Node colors from blue to orange and from small to large indicate progressively higher degree values.

Network pharmacology provides potential drug targets and pathways through computational predictions. However, it has certain limitations, as it excessively relies on network models that cannot fully capture the highly complex and dynamic nature of biological systems. The combination of network pharmacology and in *vivo* and in *vitro* experiments not only validates the accuracy of predictions but also provides deeper insights into the

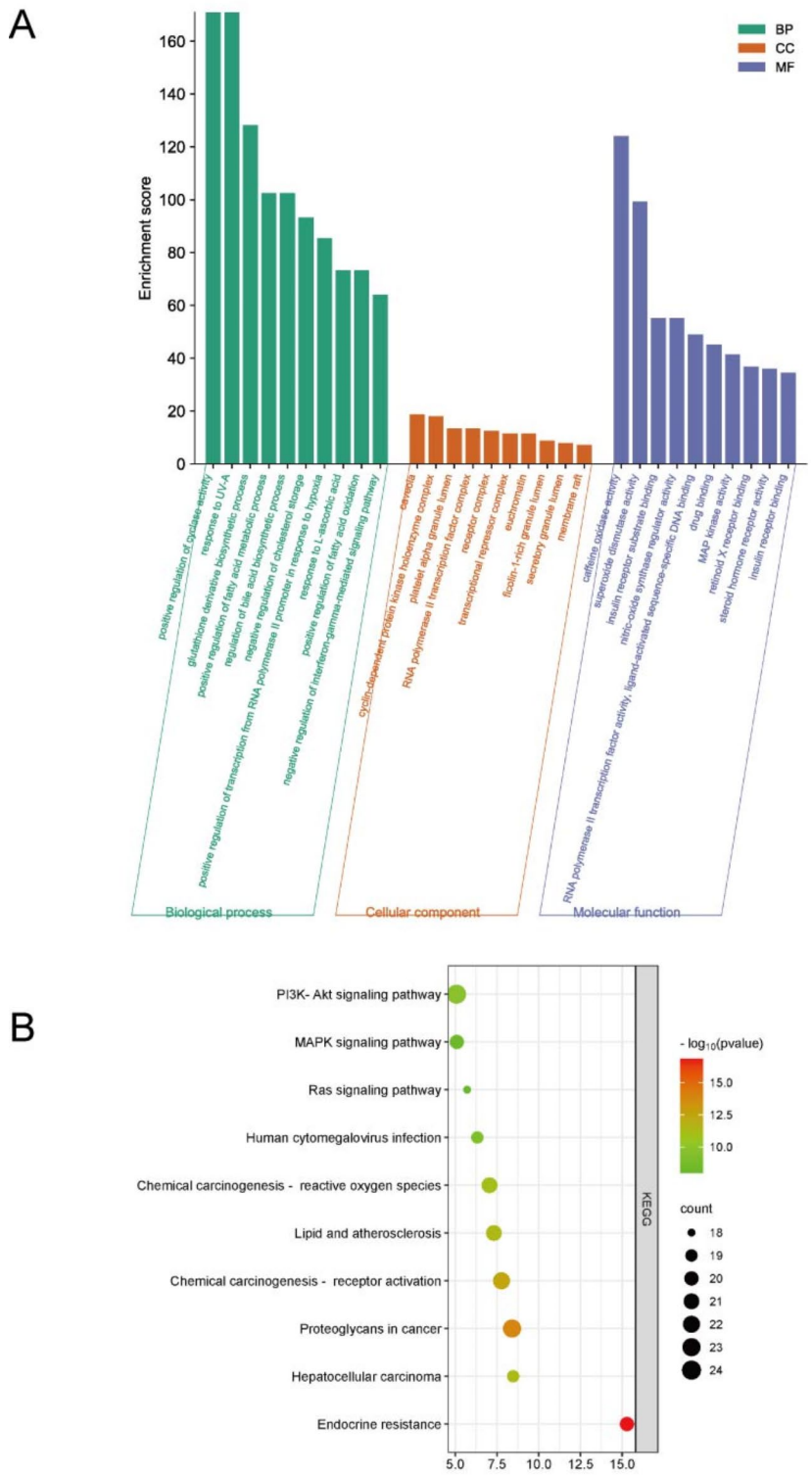

Fig. 5. GO and KEGG enrichment analyses of the overlapping targets of diosgenin in patients with NASH. (**A**) GO analysis revealed three aspects: biological process (BP), cellular component (CC), and molecular function (MF). The enriched targets were sorted in descending order according to Fold enrichment. (**B**) KEGG analysis was performed in descending order according to the number of potential targets enriched in the pathway.

multi-component and multi-target characteristics of natural products, thereby enhancing the scientific value and translational potential of the research[83,84].

In summary, this study investigated the effects and mechanisms of action of diosgenin on NASH at the systemic level through network pharmacological analysis plus cellular experimental validation. Studies suggest

ID	Biological process	*P* value	Fold enrichment	FDR
GO:0031281	Positive regulation of cyclase activity	9.97E−05	170.8672566	0.001967972
GO:0070141	Response to UV-A	9.97E−05	170.8672566	0.001967972
GO:1,901,687	Glutathione derivative biosynthetic process	1.99E−04	128.1504425	0.003474314
GO:0045923	Positive regulation of fatty acid metabolic process	3.30E−04	102.520354	0.005161332
GO:0070857	Regulation of bile acid biosynthetic process	3.30E−04	102.520354	0.005161332
GO:0010887	Negative regulation of cholesterol storage	2.70E−09	93.2003218	3.12E−07
GO:0061419	Positive regulation of transcription from RNA polymerase II promoter in response to hypoxia	4.93E−04	85.43362832	0.007379709
GO:0033591	Response to L-ascorbic acid	6.87E−04	73.22882427	0.009747128
GO:0046321	Positive regulation of fatty acid oxidation	6.87E−04	73.22882427	0.009747128
GO:0060336	Negative regulation of Interferon-gamma-mediated signaling pathway	9.13E−04	64.07522124	0.012266478

Table 3. Biological process of GO analysis.

ID	Cellular component	*P* value	Fold enrichment	FDR
GO:0005901	Caveola	2.20E−07	18.73957621	7.13E−06
GO:0000307	Cyclin-dependent protein kinase holoenzyme complex	0.001376904	18.03684211	0.012623302
GO:0031093	Platelet alpha granule lumen	5.08E−04	13.46032993	0.005663372
GO:0090575	RNA polymerase II transcription factor complex	3.48E−07	13.41583297	8.78E−06
GO:0043235	Receptor complex	1.52E−11	12.46786321	3.46E−09
GO:0017053	Transcriptional repressor complex	0.005050691	11.45196324	0.036926523
GO:0000791	Euchromatin	0.005050691	11.45196324	0.036926523
GO:1,904,813	Ficolin-1-rich granule lumen	6.14E−04	8.727504244	0.00633631
GO:0034774	Secretory granule lumen	0.003743547	7.842105263	0.03034947
GO:0045121	Membrane raft	1.07E−05	7.157477026	1.86E−04

Table 4. Cellular component of GO analysis.

ID	Molecular function	*P* value	Fold enrichment
GO:0034875	Caffeine oxidase activity	2.12E−04	124.1381579
GO:0004784	Superoxide dismutase activity	3.51E−04	99.31052632
GO:0043560	Insulin receptor substrate binding	1.58E−06	55.17251462
GO:0030235	Nitric-oxide synthase regulator activity	0.001245069	55.17251462
GO:0004879	RNA polymerase II transcription factor activity, ligand-activated sequence-specific DNA binding	1.23E−21	49.04223522
GO:0008144	Drug binding	0.001887347	45.14114833
GO:0004707	MAP kinase activity	1.11E−04	41.37938596
GO:0046965	Retinoid X receptor binding	1.60E−04	36.78167641
GO:0003707	Steroid hormone receptor activity	9.89E−06	35.98207475
GO:0005158	Insulin receptor binding	1.18E−05	34.48282164

Table 5. Molecular function of GO analysis.

that diosgenin may reduce SCD1 expression by activating the PI3K-Akt pathway in the treatment of NASH. This study lays a good foundation for further in-depth study of the mechanism of diosgenin-induced NASH and provides an important scientific basis for broader clinical application. However, further studies of the mechanism of diosgenin in the treatment of NASH are needed, and an animal model is needed for further research and exploration.

Conclusion

In this study, we employed a network pharmacology approach to investigate the effects and underlying mechanisms of diosgenin on NASH. Through screening of potential targets, construction of protein-protein interaction networks, and bioenrichment analysis, we found that diosgenin may alleviate NASH progression by enhancing fatty acid metabolism in hepatocytes via the PI3K-Akt pathway. Molecular docking results revealed that nine core targets not only exhibited strong binding affinity with diosgenin but also were reported to be associated with the PI3K-Akt pathway. Cellular experiments further confirmed our predictions, demonstrating that diosgenin reduced triglyceride accumulation and inflammatory responses in FFA-treated HepG2 cells through the PI3K-Akt pathway. This study lays a solid foundation for further exploration of the intrinsic

KEGG ID	Pathway name	Count	Enrichment	*p* value
hsa04151	PI3K-Akt signaling pathway	24	5.077904	1.38E−10
hsa05205	Proteoglycans in cancer	23	8.403312	1.50E−14
hsa05207	Chemical carcinogenesis - receptor activation	22	7.772546	3.17E−13
hsa05417	Lipid and atherosclerosis	21	7.315724	4.06E−12
hsa05208	Chemical carcinogenesis - reactive oxygen species	21	7.053277	8.02E−12
hsa01522	Endocrine resistance	20	15.28553	1.40E−17
hsa04010	MAPK signaling pathway	20	5.095176	7.61E−09
hsa05225	Hepatocellular carcinoma	19	8.47073	4.94E−12
hsa05163	Human cytomegalovirus infection	19	6.324811	6.60E−10
hsa04014	Ras signaling pathway	18	5.712642	1.02E−08

Table 6. Basic information on the first 10 signaling pathways of the KEGG pathway analysis.

Targets	PDB ID	Related parameter settings			Types of interactions	Interacting residues	Bond lengths	Binding energy(kcal/mol)
		center_x	center_y	center_z				
ALB	1N5U	29.0	10.8	15.0	Hydrogen bonds	ARG-117 ARG-186	2.5 Å 2.5 Å	− 19.4
AKT1	6NPZ	-32.3	1.2	19.3	Hydrogen bonds	LYS-179 ASP-439	2.5 Å 2.5Å	− 8.9
CASP3	4JJE	49.8	22.7	57.9	Hydrogen bonds	GLY-122	2.8 Å	− 8.4
EGFR	2GS2	68.2	18.6	-40.3	Hydrogen bonds	ASN-676 ALA-678	2.1 Å 2.6 Å	− 8.4
IGF1	1IMX	18.4	21.1	25.7	Hydrogen bonds	CYS-52	2.3 Å	− 8.0
MAPK3	4QTB	37.1	54.4	50.1	Hydrogen bonds	MET-125	2.1 Å	− 10.1
TP53	4AGP	91.8	91.9	-45.4	Hydrogen bonds	THR-231	2.7 Å	− 7.7
VEGFA	4KZN	10.4	-4.1	22.4	Hydrogen bonds	GLN-37	2.0 Å	− 8.1
STAT3	6NJS	-14.6	20.4	25.5	Hydrogen bonds	TRP-510 ASP-502	2.8 Å 2.5 Å	− 8.0

Table 7. Molecular docking parameters and results of diosgenin with target proteins. The search space dimensions are uniformly set to size_x: 60, size_y: 60, size_z: 60, with a grid spacing of 0.375 Å. The exhaustiveness parameter is fixed at 10, and all other parameters remain at their default settings.

mechanisms by which diosgenin ameliorates NASH and provides critical scientific support for its broader clinical application. As a natural compound, diosgenin holds promise as a novel therapeutic approach for NASH.

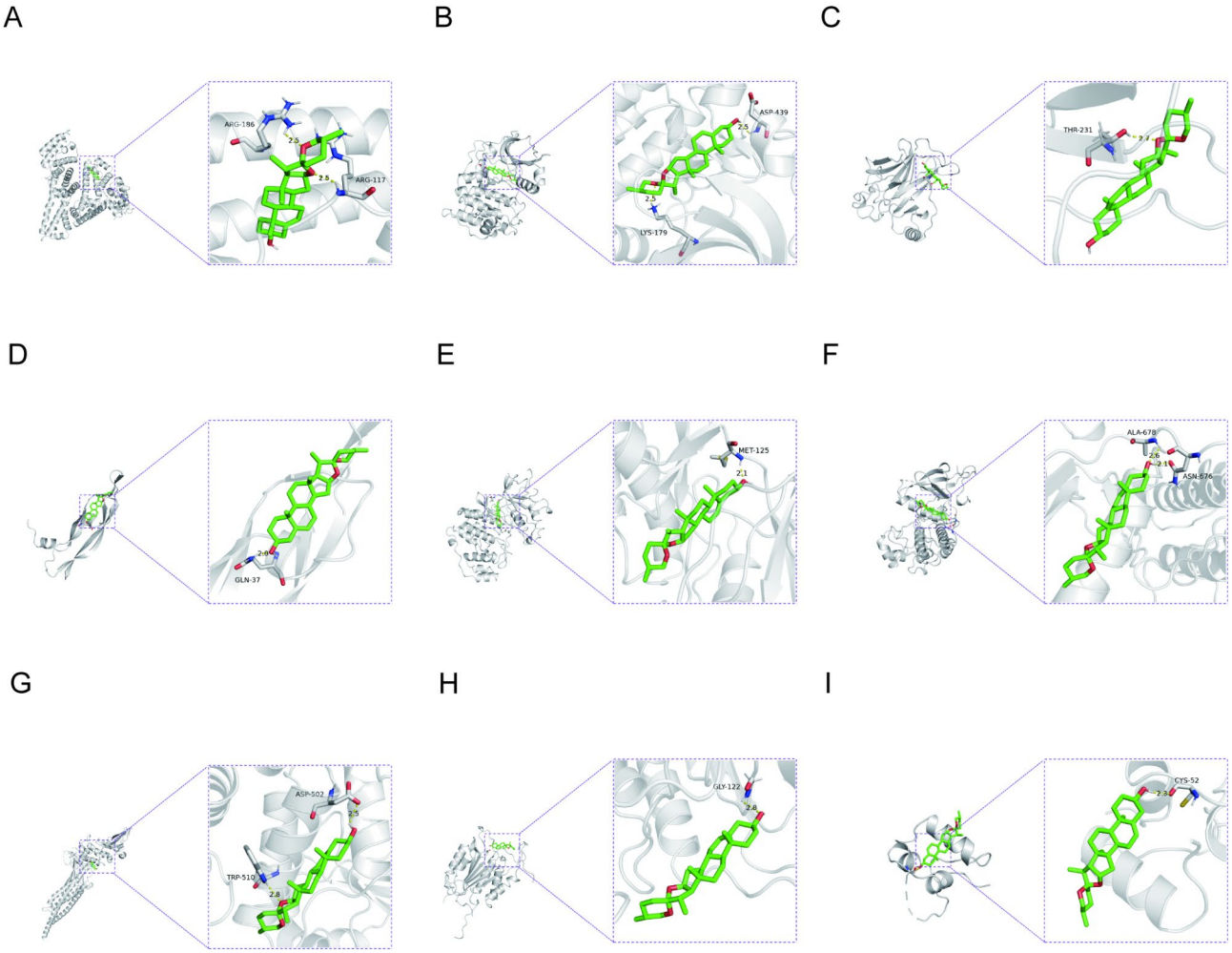

Fig. 6. The 3-dimensional map of the binding sites between diosgenin and target proteins. (**A**) ALB. (**B**) AKT1, (**C**) TP53, (**D**) VEGFA, (**E**) MAPK3, (**F**) EGFR, (**G**) STAT3, (**H**) CASP3, (**I**) IGF1. Diosgenin is shown in green. Target proteins are displayed as white. The places where diosgenin and the target proteins are connected represent specific docking sites between diosgenin and target proteins.

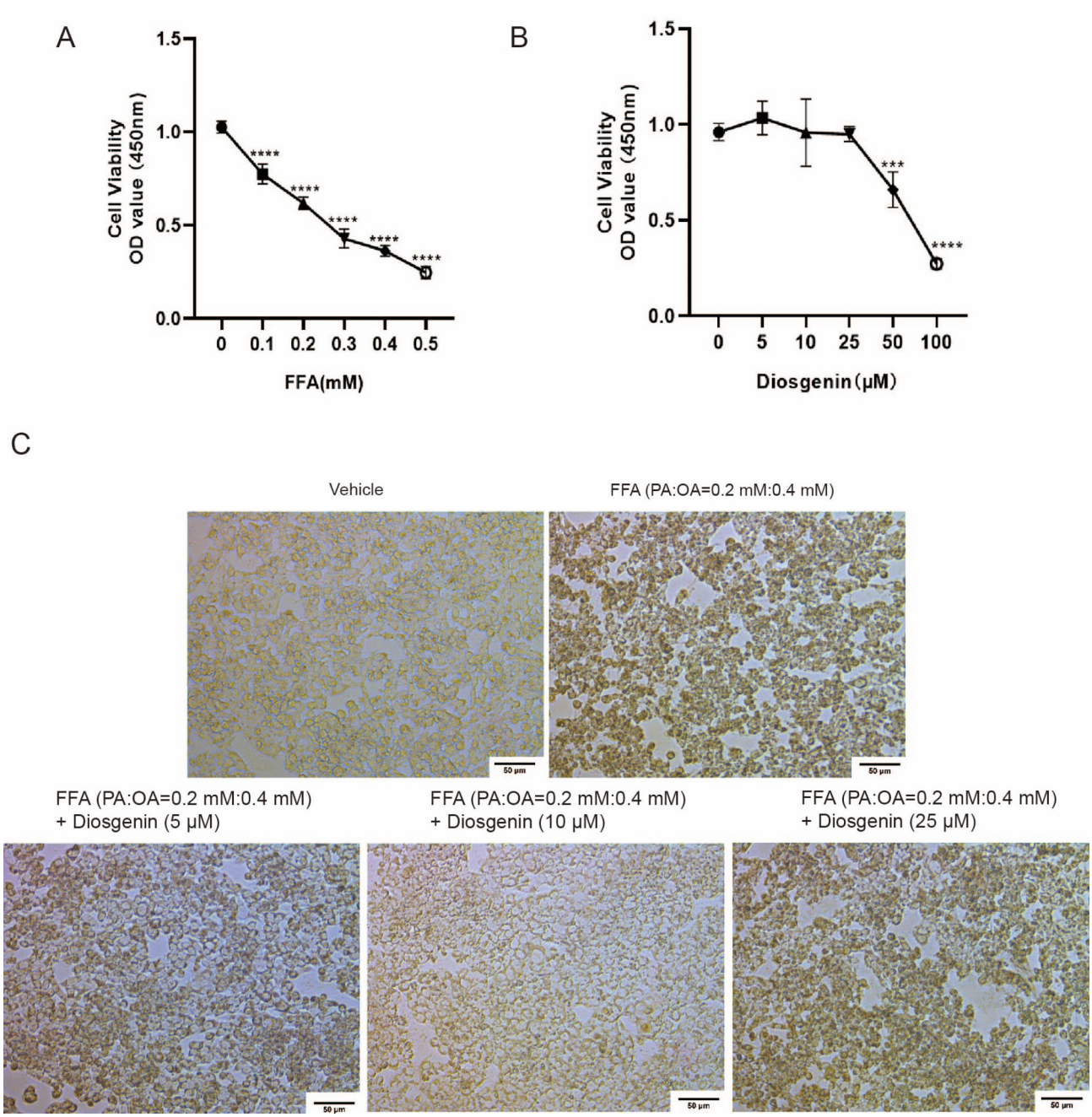

Fig. 7. Free fatty acid and diosgenin concentration screening. (**A**) Effects of different concentrations of free fatty acids (FFA, PA-to-OA molar ratio of 1:2) on cell proliferation and toxicity; (**B**) cell survival after 24 h of incubation with different concentrations of diosgenin (μM); (**C**) cell morphology of HepG2 cells in different intervention states (× 50).

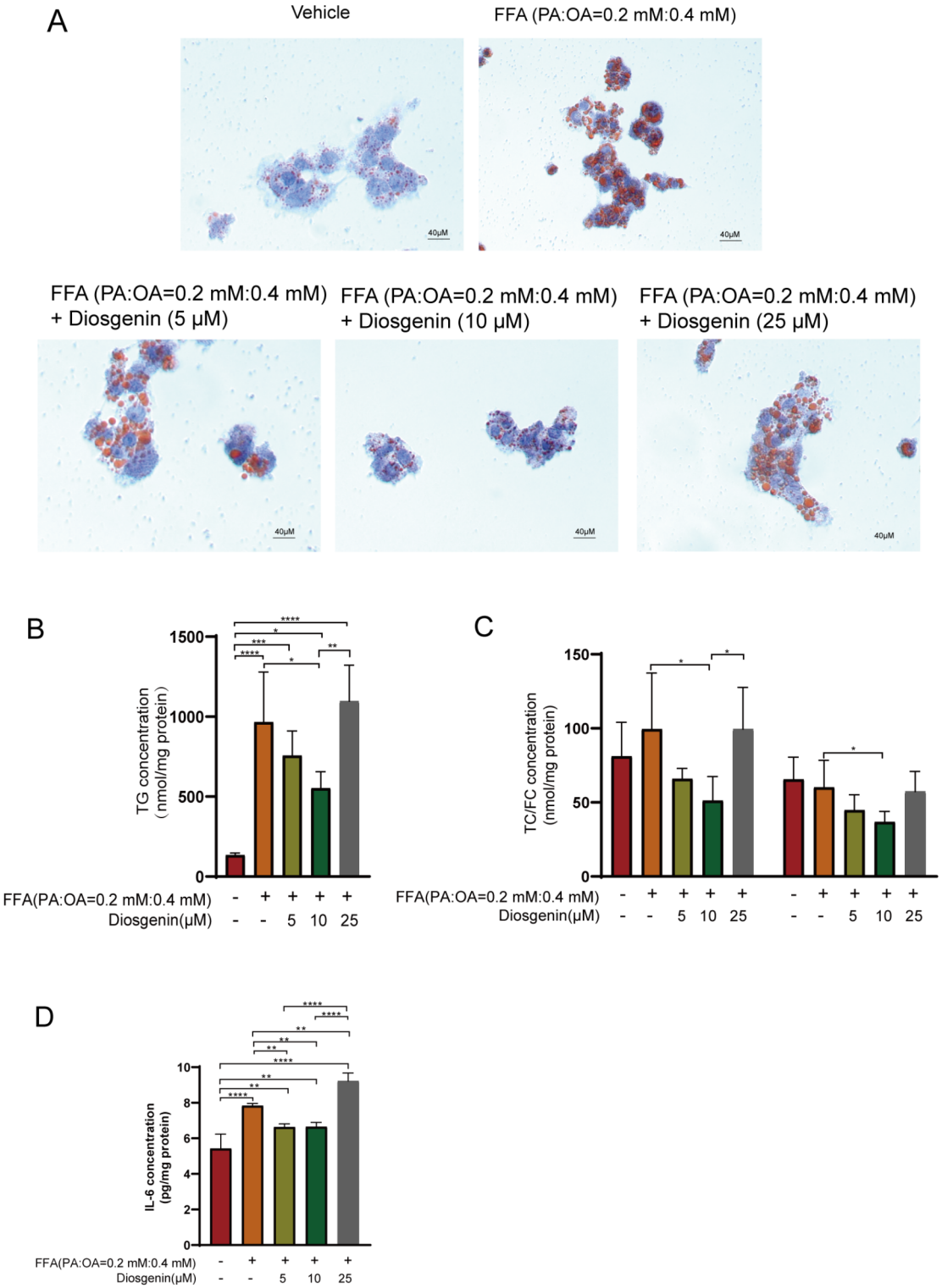

Fig. 8. Diosgenin reduces cellular triglyceride deposition and attenuates FFA-induced inflammation. (**A**) Cellular Oil Red O staining (× 40) of HepG2 cells treated with FFA and different concentrations of diosgenin. (**B**) Determination of cellular triglyceride (TG) levels in HepG2 cells treated with FFA and different concentrations of diosgenin; (**C**) Determination of cellular total cholesterol (TC) and free cholesterol (FC) levels in HepG2 cells treated with FFA and different concentrations of diosgenin; (**D**) Determination of IL-6 levels in cell culture supernatants in HepG2 cells treated with FFA and different concentrations of diosgenin; (**D**) Determination of IL-6 in cell culture supernatant after treatment of HepG2 cells with FFA and different concentrations of diosgenin. The data are expressed as the mean ± standard deviation; * indicates $P < 0.05$, ** indicates $P < 0.01$, *** indicates $P < 0.001$, and **** indicates $P < 0.0001$.

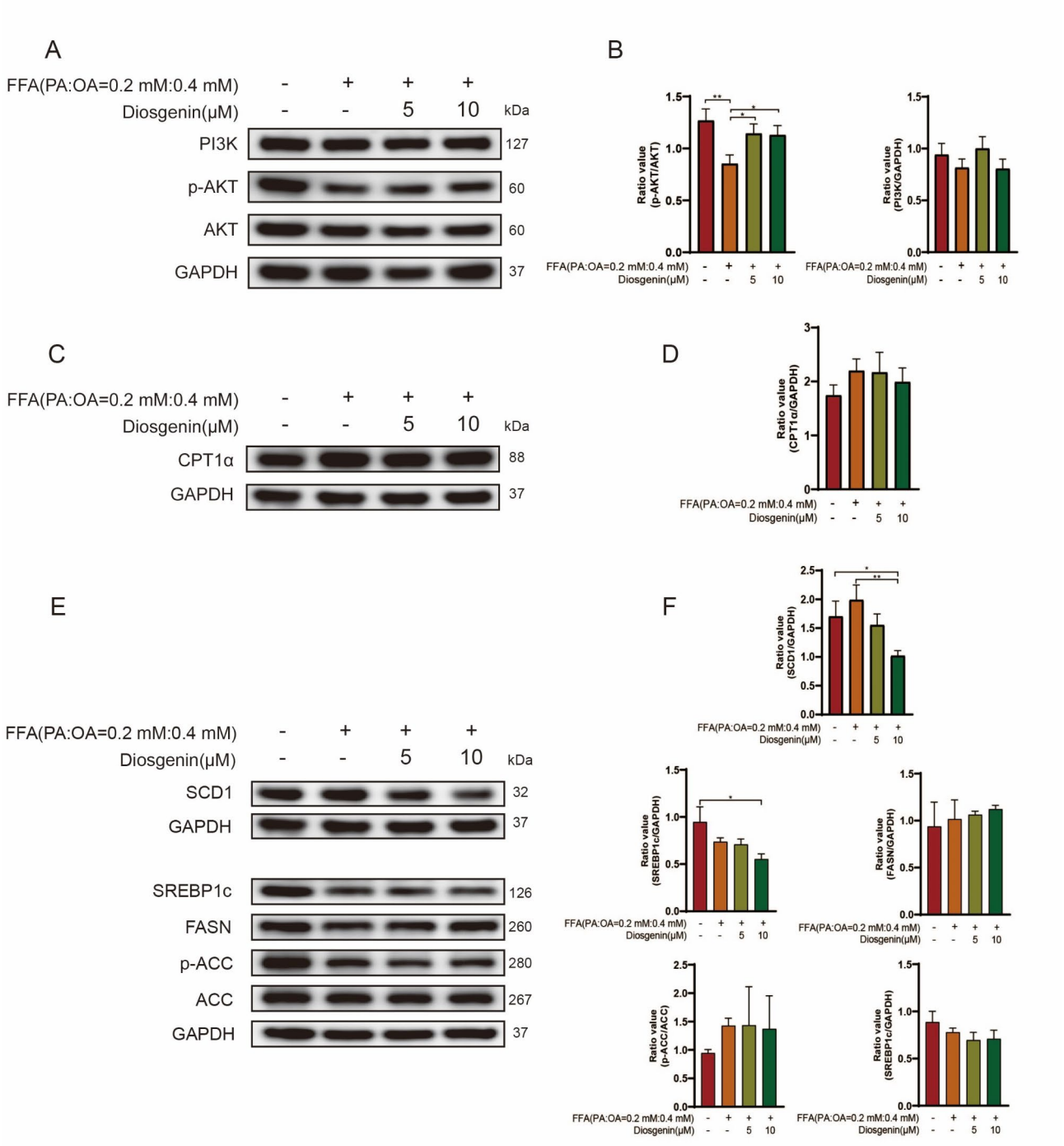

Fig. 9. Activation of the PI3K-Akt pathway by diosgenin activates lipid metabolism in hepatocytes. (**A**) Western blotting was used to detect PI3K, p-AKT, and AKT protein expression. (**C**) Western blotting was used to detect the protein expression of CPT1α, an indicator of fatty acid oxidation. (**E**) protein expression of other fatty acid metabolism-related indicators determined by Western blotting. (**B**, **D**, **F**) the data shown in the bar graphs indicate the mean ± standard deviation of three independent experiments. * indicates $P < 0.05$, ** indicates $P < 0.01$.

Data availability

Data is provided within the manuscript or supplementary information files.

Received: 9 December 2024; Accepted: 19 March 2025
Published online: 26 March 2025

References

1. Kanwal, F. et al. Preparing for the NASH epidemic: A call to action. *Gastroenterology* **161**(3), 1030–42e8 (2021).
2. Chalasani, N. et al. The diagnosis and management of nonalcoholic fatty liver disease: practice guidance from the American association for the study of liver diseases. *Hepatology* **67**(1), 328–357 (2018).
3. Sheka A C, Adeyi, O. et al. *Nonalcoholic Steatohepatitis Jama* **323**(12) (2020).
4. Bugianesi, E. Nafld/Nash. *J. Hepatol.* **77**(2), 549–550 (2022).
5. Ditah, I. C. et al. Changes in the prevalence of hepatitis C virus infection, nonalcoholic steatohepatitis, and alcoholic liver disease among patients with cirrhosis or liver failure on the waitlist for liver transplantation. *Gastroenterology* **152**(5), 1090–9e1 (2017).
6. Lambert, J. E. et al. Increased de Novo lipogenesis is a distinct characteristic of individuals with nonalcoholic fatty liver disease. *Gastroenterology* **146**(3), 726–735 (2014).
7. Kawano, Y. & Cohen, D. E. Mechanisms of hepatic triglyceride accumulation in non-alcoholic fatty liver disease. *J. Gastroenterol.* **48**(4), 434–441 (2013).
8. Koyama, Y. & Brenner, D. A. Liver inflammation and fibrosis. *J. Clin. Invest.* **127**(1), 55–64 (2017).
9. Muthiah, M. D. & Sanyal A. J. Current management of non-alcoholic steatohepatitis. *Liver Int.* **40**(Suppl 1), 89–95 (2020).
10. Harrison S A, Allen A M, Dubourg, J. et al. Challenges and opportunities in NASH drug development. *Nat. Med.* **29**(3), 562–573 (2023).
11. Li, C. et al. Vitexin ameliorates chronic stress plub high fat diet-induced nonalcoholic fatty liver disease by inhibiting inflammation. *Eur. J. Pharmacol.* **882**, 173264 (2020).
12. Wu, C. & Jing, M. Alisol A 24-acetate ameliorates nonalcoholic steatohepatitis by inhibiting oxidative stress and stimulating autophagy through the AMPK/mTOR pathway. *Chem. Biol. Interact.* **291**, 111–119 (2018).
13. Zhao, Z., Deng, Z. T., Huang, S. et al. Alisol B alleviates hepatocyte lipid accumulation and lipotoxicity via regulating RARalpha-PPARgamma-CD36 cascade and attenuates non-alcoholic steatohepatitis in mice. *Nutrients* **14**(12). (2022).
14. RAJU, J. Cancer chemopreventive and therapeutic effects of diosgenin, a food saponin. *Nutr. Cancer* **61**(1), 27–35 (2009).
15. Huang, C. H. et al. Oral administration with Diosgenin enhances the induction of intestinal T helper 1-like regulatory T cells in a murine model of food allergy. *Int. Immunopharmacol.* **42**, 59–66 (2017).
16. Kim, J. K. & Park, S. U. An update on the biological and pharmacological activities of diosgenin. *Excli J.* **17**, 24–28 (2018).
17. Gong, J. et al. Effect of Fenugreek on hyperglycaemia and hyperlipidemia in diabetes and prediabetes: A meta-analysis. *J. Ethnopharmacol.* **194**, 260–268 (2016).
18. Wu, S. et al. Dioscin improves postmenopausal osteoporosis through inducing bone formation and inhibiting apoptosis in ovariectomized rats. *Biosci. Trends* **13**(5), 394–401 (2019).
19. Li, R. et al. Diosgenin regulates cholesterol metabolism in hypercholesterolemic rats by inhibiting NPC1L1 and enhancing ABCG5 and ABCG8. *Biochim. Biophys. Acta Mol. Cell. Biol. Lipids*. **1864**(8), 1124–1133 (2019).
20. Zhang, S. Z. et al. Therapeutic potential and research progress of Diosgenin for lipid metabolism diseases. *Drug Dev. Res.* **83**(8), 1725–1738 (2022).
21. Sun, F. & Yang, X. The effects of Diosgenin on hypolipidemia and its underlying mechanism: A review. *Diabetes Metab. Syndr. Obes.* **14**, 4015–4030 (2021).
22. Cheng, S. et al. Diosgenin prevents high-fat diet-induced rat non-alcoholic fatty liver disease through the AMPK and LXR signaling pathways. *Int. J. Mol. Med.* **41**(2), 1089–1095 (2018).
23. Yan, M. et al. Diosgenin alleviates nonalcoholic steatohepatitis through affecting liver-gut circulation. *Pharmacol. Res.*, 187 (2023).
24. Hirai, S. et al. Diosgenin attenuates inflammatory changes in the interaction between adipocytes and macrophages. *Mol. Nutr. Food Res.* **54**(6), 797–804 (2010).
25. Khateeb, S. & Albalawi, A. Diosgenin modulates oxidative stress and inflammation in high-fat diet-induced obesity in mice. *Diabetes Metab. Syndr. Obes.* **15**, 1589–1596 (2022).
26. Nogales, C. et al. Network pharmacology: Curing causal mechanisms instead of treating symptoms. *Trends Pharmacol. Sci.* **43**(2), 136–150 (2022).
27. Lai, X. et al. Editorial: Network pharmacology and traditional medicine. *Front. Pharmacol.* **11**, 1194 (2020).
28. Fang, S. et al. HERB: A high-throughput experiment- and reference-guided database of traditional Chinese medicine. *Nucleic Acids Res.* **49**(D1), D1197–d206 (2021).
29. Kim, S. et al. PubChem in 2021: New data content and improved web interfaces. *Nucleic Acids Res.* **49**(D1), D1388–d95 (2021).
30. Wang, X. et al. Enhancing the enrichment of pharmacophore-based target prediction for the polypharmacological profiles of drugs. *J. Chem. Inf. Model.* **56**(6), 1175–1183 (2016).
31. Wang, X. et al. PharmMapper 2017 update: A web server for potential drug target identification with a comprehensive target pharmacophore database. *Nucleic Acids Res.* **45**(W1), W356–w60 (2017).
32. Daina, A. & Michielin, O. SwissTargetPrediction: Updated data and new features for efficient prediction of protein targets of small molecules. *Nucleic Acids Res.* **47**(W1), W357–w64 (2019).
33. UniProt. A worldwide hub of protein knowledge. *Nucleic Acids Res.* **47**(D1), D506–d15 (2019).
34. Stelzer, G. et al. The GeneCards Suite: From gene data mining to disease genome sequence analyses. *Curr. Protoc. Bioinform.* **54** 1.30.1–1.3 (2016).
35. PIñero, J. et al. The disgenet knowledge platform for disease genomics: 2019 update. *Nucleic Acids Res.* **48**(D1), D845–d55 (2020).
36. Boyadjiev, S. A. & Jabs E. W. Online Mendelian inheritance in man (OMIM) as a knowledgebase for human developmental disorders. *Clin. Genet.* **57**(4), 253–266 (2000).
37. Chen, X. et al. Therapeutic target database. *Nucleic Acids Res.* **30**(1), 412–415 (2002).
38. LUO, W. Pathview: An R/Bioconductor package for pathway-based data integration and visualization. *Bioinformatics* **29**(14), 1830–1831 (2013).
39. Huang Da, W., Sherman, B. T., Lempicki, R. A. Systematic and integrative analysis of large gene lists using DAVID bioinformatics resources. *Nat. Protoc.* **4**(1), 44–57 (2009).
40. Shi, L. et al. Gene expression profiling and functional analysis reveals that p53 pathway-related gene expression is highly activated in cancer cells treated by cold atmospheric plasma-activated medium. *PeerJ* **5**, e3751 (2017).
41. Szklarczyk, D. et al. The STRING database in 2017: Quality-controlled protein-protein association networks, made broadly accessible. *Nucleic Acids Res.* **45**(D1), D362–d8 (2017).
42. Ru, J. et al. TCMSP: A database of systems Pharmacology for drug discovery from herbal medicines. *J. Cheminform.* **6**, 13 (2014).
43. Shannon, P. et al. Cytoscape: a software environment for integrated models of biomolecular interaction networks. *Genome Res.* **13**(11), 2498–2504 (2003).
44. Wang, C. et al. PI3K-AKT-mediated phosphorylation of Thr260 in CgCaspase-3/6/7 regulates heat-induced activation in oysters. *Commun. Biol.* **7**(1), 1459 (2024).
45. Bao, X. Exploring the protective mechanism of Gankang tablets on liver function in rats with carbon tetrachloride-induced liver fibrosis based on PI3K/Akt signaling pathway. *Mod. Dig. Interv. Diagn.Treat.* **25**(02), 188–192 (2020).
46. Alvarado-ortiz, E. et al. Mutant p53 gain-of-function stimulates canonical Wnt signaling via PI3K/AKT pathway in colon cancer. *J. Cell. Commun. Signal.* **17**(4), 1389–1403 (2023).
47. Dai, W. et al. Human umbilical cord-derived mesenchymal stem cells (hUC-MSCs) alleviate excessive autophagy of ovarian granular cells through VEGFA/PI3K/AKT/mTOR pathway in premature ovarian failure rat model. *J. Ovarian Res.* **16**(1), 198 (2023).

48. Prochazka, R. et al. The role of MAPK3/1 and AKT in the acquisition of high meiotic and developmental competence of Porcine oocytes cultured in vitro in FLI medium. *Int. J. Mol. Sci.* **22**(20) (2021).
49. Novoplansky, O., Shnerb, A. B., Marripati, D. et al. Activation of the EGFR/PI3K/AKT pathway limits the efficacy of Trametinib treatment in head and neck cancer. *Mol. Oncol.* **17**(12), 2618–2636 (2023).
50. Sun, Z. & Jiang, Q. AKT blocks SIK1-mediated repression of STAT3 to promote breast tumorigenesis. *Cancer Res.* **83**(8), 1264–1279 (2023).
51. Zhao, J. et al. CircCCDC91 regulates chicken skeletal muscle development by sponging miR-15 family via activating IGF1-PI3K/AKT signaling pathway. *Poult. Sci.* **101**(5), 101803 (2022).
52. Shi, H. et al. Baicalin attenuates hepatic injury in non-alcoholic steatohepatitis cell model by suppressing inflammasome-dependent GSDMD-mediated cell pyroptosis. *Int. Immunopharmacol.* **81**, 106195 (2020).
53. Heron-Milhavet, L. & Khouya, N. Akt1 and Akt2: Differentiating the Aktion. *Histol. Histopathol.* **26**(5), 651–662 (2011).
54. Vivanco I. & Sawyers, C. L. The phosphatidylinositol 3-Kinase AKT pathway in human cancer. *Nat. Rev. Cancer* **2**(7), 489–501 (2002).
55. Yoeli-Lerner, M. et al. Akt blocks breast cancer cell motility and invasion through the transcription factor NFAT. *Mol. Cell.* **20**(4), 539–550 (2005).
56. Chen, W. S. et al. Growth retardation and increased apoptosis in mice with homozygous disruption of the Akt1 gene. *Genes Dev.* **15**(17), 2203–2208 (2001).
57. Cho, H. et al. Akt1/PKBalpha is required for normal growth but dispensable for maintenance of glucose homeostasis in mice. *J. Biol. Chem.* **276**(42), 38349–38352 (2001).
58. Abeyrathna, P. & su, Y. The critical role of Akt in cardiovascular function. *Vascul Pharmacol.* **74**, 38–48 (2015).
59. Liu, G. et al. BRG1 regulates lipid metabolism in hepatocellular carcinoma through the PIK3AP1/PI3K/AKT pathway by mediating GLMP expression. *Dig. Liver Dis.* **54**(5), 692–700 (2022).
60. Liao, X. et al. LAMP3 regulates hepatic lipid metabolism through activating PI3K/Akt pathway. *Mol. Cell. Endocrinol.* **470**, 160–167 (2018).
61. Cui, X. et al. Scutellariae radix and coptidis rhizoma improve glucose and lipid metabolism in T2DM rats via regulation of the metabolic profiling and MAPK/PI3K/Akt signaling pathway. *Int. J. Mol. Sci.*, **19**(11). (2018).
62. Li, A. et al. PTX3/TWIST1 feedback loop modulates Lipopolysaccharide-Induced inflammation via PI3K/Akt signaling pathway. *J. Interferon Cytokine Res.* **42**(4), 161–169 (2022).
63. Sun, X., Chen, L. & He, Z. PI3K/Akt-Nrf2 and Anti-Inflammation effect of macrolides in chronic obstructive pulmonary disease. *Curr. Drug Metab.* **20**(4), 301–304 (2019).
64. He, M. et al. Defect in Ser312 phosphorylation of Tp53 dysregulates lipid metabolism for fatty accumulation and fatty liver susceptibility: Revealed by lipidomics. *J. Chromatogr. B Analyt Technol. Biomed. Life Sci.* **1211**, 123491 (2022).
65. Shen, H. et al. Hepatocyte-derived VEGFA accelerates the progression of non-alcoholic fatty liver disease to hepatocellular carcinoma via activating hepatic stellate cells. *Acta Pharmacol. Sin.* **43**(11), 2917–2928 (2022).
66. Guéguinou, M. et al. Lipid rafts, KCa/ClCa/Ca2 + channel complexes and EGFR signaling: novel targets to reduce tumor development by lipids?. *Biochim. Biophys. Acta* **1848**(10 Pt B), 2603–2620 (2015).
67. Kinoshita, S. et al. Role of hepatic STAT3 in the regulation of lipid metabolism. *Kobe J. Med. Sci.* **54**(4), E200–E208 (2008).
68. Ma, X. Y. et al. Ursolic acid reduces hepatocellular apoptosis and alleviates alcohol-induced liver injury via irreversible Inhibition of CASP3 in vivo. *Acta Pharmacol. Sin.* **42**(7), 1101–1110 (2021).
69. Fukunaga, K. et al. IGF1 suppresses cholesterol accumulation in the liver of growth hormone-deficient mice via the activation of ABCA1. *Am. J. Physiol. Endocrinol. Metab.* **315**(6), E1232–e41 (2018).
70. Sethi, G. et al. Pro-apoptotic and anti-cancer properties of diosgenin: A comprehensive and critical review. *Nutrients* **10**(5) (2018).
71. Lv, Y. C., Yang, J., Yao, F. et al. Diosgenin inhibits atherosclerosis via suppressing the MiR-19b-induced downregulation of ATP-binding cassette transporter A1. *Atherosclerosis* **240**(1), 80–89 (2015).
72. Kim, J. E. et al. Diosgenin effectively suppresses skin inflammation induced by phthalic anhydride in IL-4/Luc/CNS-1 transgenic mice. *Biosci. Biotechnol. Biochem.* **80**(5), 891–901 (2016).
73. Chiang, S. S., Chang, S. P. & Pan, T. M. Osteoprotective effect of *Monascus*-fermented *Dioscorea* in ovariectomized rat model of postmenopausal osteoporosis. *J. Agric. Food Chem.* **59**(17), 9150–9157 (2011).
74. Chen, Y. et al. Advances in the pharmacological activities and mechanisms of diosgenin. *Chin. J. Nat. Med.* **13**(8), 578–587 (2015).
75. Basch, E. et al. Therapeutic applications of fenugreek. *Altern. Med. Rev.* **8**(1), 20–27 (2003).
76. Wang, T. et al. Antihyperlipidemic effect of protodioscin, an active ingredient isolated from the rhizomes of *Dioscorea Nipponica*. *Planta Med.* **76**(15), 1642–1646 (2010).
77. Am, A. L., Syed, D. N. & Ntambi, J. M. Insights into stearoyl-CoA desaturase-1 regulation of systemic metabolism. *Trends Endocrinol. Metab.* **28**(12), 831–842 (2017).
78. Ntambi, J. M. et al. Loss of stearoyl-CoA desaturase-1 function protects mice against adiposity. *Proc. Natl. Acad. Sci. U S A* **99**(17), 11482–11486 (2002).
79. Sampath, H. & Ntambi, J. M. The role of stearoyl-CoA desaturase in obesity, insulin resistance, and inflammation. *Ann. N Y Acad. Sci.* **1243**, 47–53 (2011).
80. Miyazaki, M. et al. Hepatic stearoyl-CoA desaturase-1 deficiency protects mice from carbohydrate-induced adiposity and hepatic steatosis. *Cell. Metab.* **6**(6), 484–496 (2007).
81. Lee, J. J. et al. Palmitoleic acid is elevated in fatty liver disease and reflects hepatic lipogenesis. *Am. J. Clin. Nutr.* **101**(1), 34–43 (2015).
82. Karami-Mohajeri, S. et al. Diosgenin: Mechanistic insights on its anti-inflammatory effects. *Antiinflamm. Antiallergy Agents Med. Chem.* **21**(1), 2–9 (2022).
83. Li, S. et al. Suppressive effects of a Chinese herbal medicine qing-luo-yin extract on the angiogenesis of collagen-induced arthritis in rats. *Am. J. Chin. Med.* **31**(5), 713–720 (2003).
84. Wang, Z. Y. et al. Mechanism of action of daqinjiao decoction in treating cerebral small vessel disease explored using network pharmacology and molecular docking technology. *Phytomedicine* **108**, 154538 (2023).

Author contributions

P.Y.G.: Writing—original draft, Validation, Data curation, Visualization. J.C.: Writing—original draft, Methodology, Investigation, Data curation. J.X.X.: Methodology, Data curation, Validation. H.Q.C.: Investigation, Validation. R.Z.: Methodology, Formal analysis. D.C.: Formal analysis, Investigation. Y.H.Z.: Writing—review & editing, Methodology, Resources, Supervision. S.S.S.: Writing—review & editing, Supervision, Funding acquisition, Resources, Conceptualization. All authors reviewed the manuscript.

Funding

This work was supported by the National Natural Science Foundation (82070818 and 82370868), Taishan Scholar Project of Shandong Province (tsqn202211330), the Natural Science Foundation of Shandong Province

(ZR2024MH086, ZR2020MH037), together with Postdoctoral Innovation Project of Shandong Province (SDCX-ZG-202203058).

Declarations

Competing interests
The authors declare no competing interests.

Additional information
Supplementary Information The online version contains supplementary material available at https://doi.org/10.1038/s41598-025-95154-z.

Correspondence and requests for materials should be addressed to Y.Z. or S.S.